Radboud Repository

Radboud University Nijmegen

PDF hosted at the Radboud Repository of the Radboud University Nijmegen

The following full text is a preprint version which may differ from the publisher's version.

For additional information about this publication click this link.
http://hdl.handle.net/2066/122723

Please be advised that this information was generated on 2017-12-05 and may be subject to change.

REVIEW ARTICLE

Towards the event horizon - the supermassive black hole in the Galactic Center

H Falcke[1,2,3] and S B Markoff[4]

[1] Department of Astrophysics, Institute for Mathematics, Astrophysics and Particle Physics (IMAPP), Radboud University Nijmegen, P.O. Box 9010, 6500 GL Nijmegen, The Netherlands
[2] ASTRON, Oude Hoogeveensedijk 4, 7991 PD Dwingeloo, The Netherlands
[3] Max-Planck-Institut für Radioastronomie, Auf dem Hügel 69, 53121 Bonn, Germany
[4] Astronomical Institute 'Anton Pannekoek', University of Amsterdam, Postbus 94249, 1090 GE Amsterdam, The Netherlands

E-mail: h.falcke@astro.ru.nl, s.b.markoff@uva.nl

Abstract. The center of our Galaxy hosts the best constrained supermassive black hole in the universe, Sagittarius A* (Sgr A*). Its mass and distance have been accurately determined from stellar orbits and proper motion studies, respectively, and its high-frequency radio, and highly variable near-infrared and X-ray emission originate from within a few Schwarzschild radii of the event horizon. The theory of general relativity (GR) predicts the appearance of a black hole shadow, which is a lensed image of the event horizon. This shadow can be resolved by very long baseline radio interferometry and test basic predictions of GR and alternatives thereof. In this paper we review our current understanding of the physical properties of Sgr A*, with a particular emphasis on the radio properties, the black hole shadow, and models for the emission and appearance of the source. We argue that the Galactic Center holds enormous potential for experimental tests of black hole accretion and theories of gravitation in their strong limits.

1. Black holes in astrophysics

The defining feature which distinguishes black holes from any other physical object is the event horizon. This one-way membrane in the fabric of spacetime defines not only the boundary between regions that are causally disconnected, but it is also the border where time and space exchange their nature. However, can one experimentally demonstrate that an event horizon exists?

Black hole candidates come in two fundamental mass classes: stellar black holes, which are essentially the collapsed cores of massive stars that either first exploded as supernovae or directly collapsed, and supermassive black holes (SMBHs), which reside in the nuclei of most, if not all, galaxies. If M_{bh} is the mass of the black hole, its characteristic scale is set by the size of the event horizon in the non-spinning case, the Schwarzschild radius $R_{\mathrm{S}} = 2GM_{\mathrm{BH}}/c^2 \sim 3$ km $(M_{\mathrm{bh}}/M_{\odot})$, where G is the gravitational constant, c is the speed of light, and $M_{\odot} = 2 \times 10^{30}$ kg is the mass of the sun. Stellar-mass black holes have masses of order $10 M_{\odot}$ and thus sizes of several tens of kilometers. They are typically found at distances of a few kpc (1 kpc = 1000 pc = 3×10^{16} km). There could be up to 10^8 stellar BHs in our Galaxy [1, 2], of which only some 10^5 would be in binaries using estimates — based on typical duty cycles and the few hundred that have actually been detected [3].

Supermassive black holes have masses between $\sim 10^6 - 10^{10} M_{\odot}$ and can be detected in galaxies from Mpc to Gpc distances. The angular size of R_{S} for a black hole at distance D is $\theta_{\mathrm{RS}} = 0.1$ nanoarcsec $(M_{\mathrm{bh}}/10 M_{\odot})(\mathrm{kpc}/D)$. For stellar mass black holes, R_{S} lies well below the resolution capabilities of any current technology. Although SMBHs are intrinsically much bigger they are also much further away, which makes their angular size generally also too small to be resolved by any telescope.

Hence, it is worthwhile to turn to the center of our own Galaxy, which hosts the closest candidate SMBH. Here, telescopes are able to resolve the gravitational sphere of influence‡ and the outer accretion region of the central source so that many basic parameters can be constrained — some to the second digit, others within an order of magnitude, but always with a level of confidence that is often impossible to achieve for more distant objects. It is here where we can hope to develop an ideal "Laboratory for Magnetohydrodynamics and General Relativity" [4].

2. The black hole in the Galactic Center: observational properties

Based on observations of other active SMBHs (also called Active Galactic Nuclei; AGN), Lynden-Bell & Rees [5] already proposed in 1971 to look for a compact radio source in the center of our own Milky Way, which was then indeed discovered three years later by the NRAO interferometer at Green Bank [6] and then by Westerbork [7]. This "compact radio source in the Galactic Center" became later known as "Sagittarius A*" (Sgr A*)

‡ The region where the gravitational potential of the BH dominates over the potential due to stars.

and by now is the best constrained SMBH candidate we know of (see [8, 9, 10, 11] for reviews and [12] for a textbook).

What makes Sgr A* so special is its proximity at only 8 kpc, coupled with its large mass of about 4 million solar masses, yielding $\theta_{RS} = 10$ μas. In fact, Sgr A*'s visible event horizon, affected by lensing in it own gravitational potential, is predicted to be $\sim 5\theta_{RS} \simeq 50$ μas [13], subtending the largest angle on the sky compared to any other black hole in the universe [14].

2.1. Mass of Sgr A*

Particularly unique is how accurately the mass of Sgr A* has been determined. Since optical radiation from the Galactic Center is completely absorbed§, the only observing bands where Sgr A* is clearly detected are radio (including sub-mm waves), the near- and mid- infrared (NIR/MIR), and X-rays.

The first evidence for a central dark mass of a few million solar masses came from the MIR (e.g., [16, 17]) and radio recombination line observations of gas streamers around Sgr A* [18, 19]. The final breakthrough, however, came with the development of adaptive optics for ground-based facilities. This provided very high spatial resolution and the ability to detect individual stars in orbit around Sgr A* [20]. After it was demonstrated that proper motions of stars could be detected [21, 22], various groups have been following the motions of individual stars over several decades and have used them to map out the gravitational potential within which they move (e.g., [23, 24, 25, 26]). These stars show textbook-like Keplerian elliptical orbits (Figure 1), with orbital speeds reaching up to 10,000 km s^{-1} and orbital periods as short as 12-16 years [27, 28, 29].

These studies show that indeed the gravitational potential in the central parsec of the Milky Way must be dominated by a single point source of mass $M_{BH} = 4.3(\pm0.4) \times 10^6 M_\odot$ [25, 26], which is concentrated within a few hundred R_S of Sgr A*. The limiting factor is the precise localization of Sgr A* within the NIR coordinate frame [30] and is only good to within ~ 2 mas (see Table 4 in [26]; mas = milliarcsecond), i.e., $\sim 200\,R_s$.

Radial velocities for many stars can be determined from high-resolution spectroscopy. Combined with proper motions of the same stars this yields a geometric distance measure of $D = 8.3(\pm0.4)$ kpc [31, 25, 26]. The longterm astrometric accuracy of these observations can be as good as 0.15-0.3 mas = 15-30 R_s. Nonetheless, the distance uncertainty still provides a significant source of systematic uncertainty for the mass. Most recent VLBA observations of many masers in the Galaxy yield a Galactic Center distance of $D = 8.35(\pm0.15)$ kpc [32], consistent with the position of Sgr A* and providing smaller error bars.

§ Meaning that the true location of the Galactic Center was unknown until it was detected by radio telescopes in the 1950s, which then led to a significant revision of the Galactic coordinate system by $> 30°$ in latitude [15]. Still today the official origin of the Galactic Center is slightly offset from the black hole.
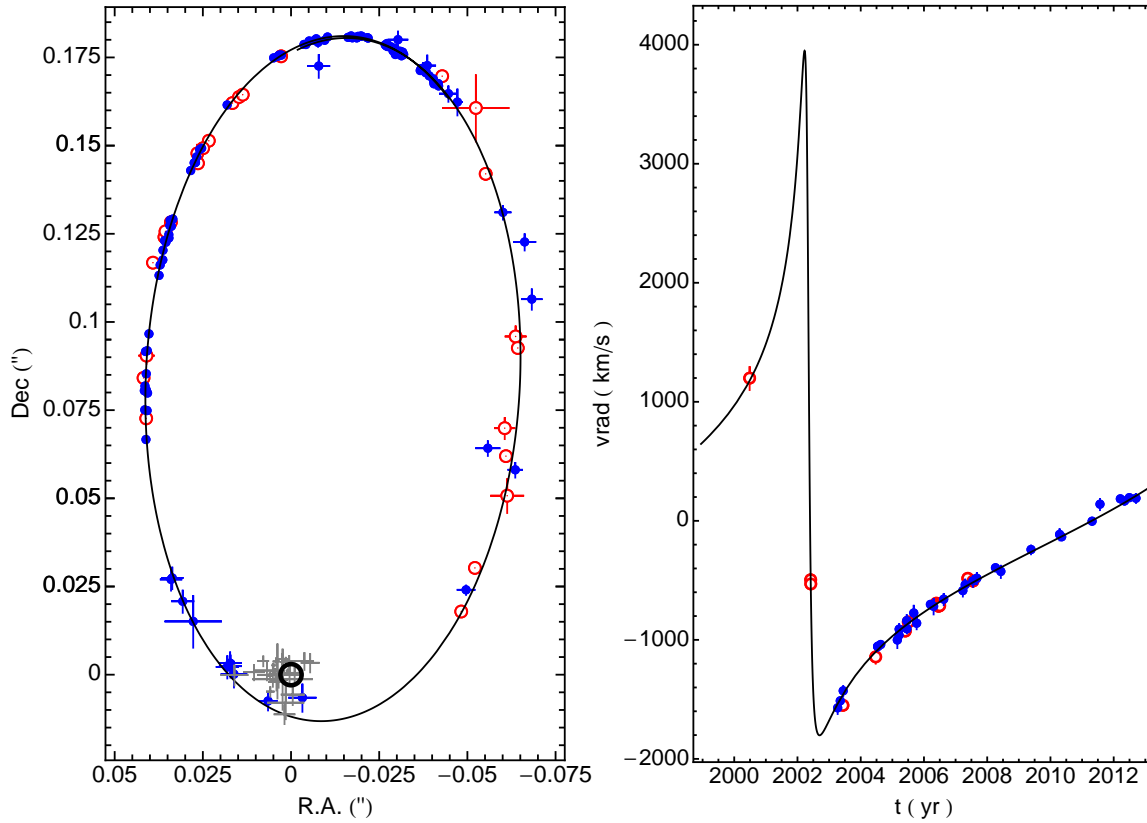
Figure 1 Measured locations and fitted orbit of the star S2 around Sgr A* (left) and its radial velocity (right), taken from Genzel, Eisenhauer, & Gillessen [10]. The radio position of Sgr A* is marked by a black circle and NIR flares from Sgr A* by grey crosses. Blue, filled circles denote the NTT/VLT points of Gillessen et al. (2009a,b, updated to 2010), and open and filled red circles are the Keck data of Ghez et al. (2008) corrected for the difference in coordinate system definition (Gillessen et al. 2009a).

The final piece of evidence for the association of a dark mass with Sgr A* comes from its own proper motion. Very long baseline interferometry (VLBI) using radio telescopes has been able to track the position of the source over several years to within a fraction of a mas per epoch [33, 34]. Sgr A*'s motion on the sky is entirely consistent with the solar system motion around the center of the Galaxy, i.e., the radio source is indeed in the Galactic Center and not in the fore- or background, and any motion perpendicular to the projected motion is $< 0.4(\pm 0.9)$ km/sec. Compared to the high velocities of stars, this implies that more than 10%, if not all, of the dark mass is indeed associated with the radio source.

2.2. Spectrum of Sgr A*

The apparent size and emission spectrum of Sgr A* are intimately linked and are crucial for understanding the source as a whole.
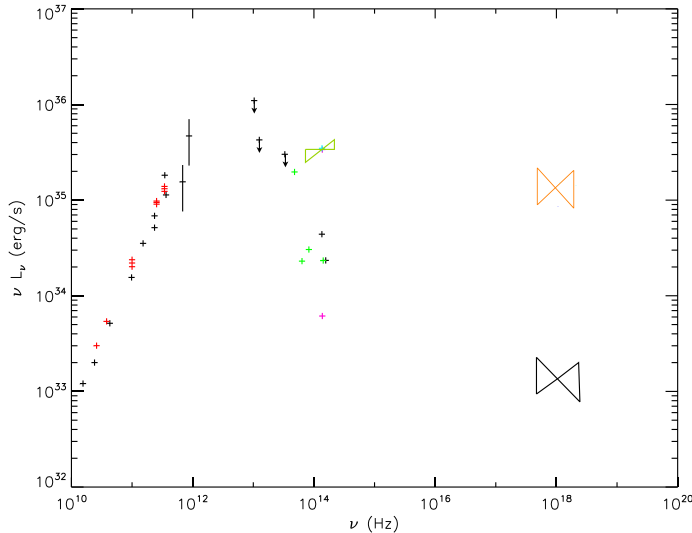
Figure 2 Broad-band spectrum of Sgr A* compiled by [35], showing both the quiescent and flaring states. The black data points represent an average spectrum, compiled from [36], [37], with NIR upper limits from [38] and [39]. The black X-ray bowtie is dominated by the outer accretion flow on scales of the Bondi radius [40], likely containing a $\sim 10\%$ contribution to this flux from Sgr A* itself [41]. The red radio data are taken from ALMA (Brinkerink & Falcke, in prep.). The green IR data points are from [42], and the pink and cyan representative IR lower/upper limits are taken from [43], [44], and [45]. The green bowtie is from [46], and is one of the few IR detections with a slope determination that is simultaneous with an X-ray detection. The orange bowtie is from the largest X-ray flare detected so far with *Chandra* [47], and the (dark/light) blue data points are two flares observed with NuSTAR [48]. NuStar data is not available in the arXiv version.

Combining all radio data on Sgr A* one finds that the radio flux density S_ν, shows a flat-to-inverted spectrum, i.e., it rises slowly with frequency with the power peaking around 10^{12} Hz in the submm band. Figure 2 shows the broad-band spectrum of Sgr A* as $\nu \times L_\nu$, where $L_\nu = 4\pi D_{\mathrm{Sgr\ A*}}^2 S_\nu$. This frequently used representation shows the power flux, and means that the flat radio spectrum becomes steeply rising in such a plot.. At GHz frequencies one has $S_\nu \propto \nu^\alpha$ and $\alpha \sim 0.3 \pm 0.1$ (which becomes ~ 1.3 in a νL_ν plot). The spectrum continues towards low frequencies ($\sim$300 MHz) with no sign of absorption [49, 50].

At higher frequencies the spectrum extends into the sub-THz (i.e., sub-mm wavelength) regime [51, 52, 38, 36], where the spectrum peaks and then suddenly cuts-off. The so-called "submm bump" is due to synchrotron emission in transition from being optically thick to thin, and simple arguments demonstrate that this emission can only arise from the most compact regions several R_{S} in diameter [36]. For self-

absorbed synchrotron sources, higher frequencies are typically emitted at smaller scales, and suspiciously the high-frequency peak in the spectrum of Sgr A* implies a scale on the order of the event horizon [53]. Hence, it was argued [36] that the event horizon of Sgr A* could be imaged against the "background" of this emission, using VLBI at sub-mm wavelengths ("submm-VLBI").

2.3. Size and structure of Sgr A*

One of the first "disappointments" of interferometric measurements of Sgr A* was that the measured source size and structure were not intrinsic to the source itself. The shape of Sgr A* is blurred into an east-west oriented ellipse of axial ratio 2:1 caused by scattering of the radio waves by electrons in the interstellar medium between us and the Galactic Center [54, 55, 56, 57]. Interestingly, recent data from a similarly scattered pulsar near Sgr A* [58, 59] suggest that the location of this scattering screen is actually not directly in the Galactic center [60]. The observed size of Sgr A* follows a λ^2 law, such that the scatter-broadened angular size is ([61], see also Figure 3, left)

$$\phi_{\text{scatt}} = (1.36 \pm 0.02)\,\text{mas} \times (\lambda/\text{cm})^2. \tag{1}$$

Using a closure amplitude technique, however, Bower et al. [62] found that at 43 and 22 GHz the measured sizes actually deviate slightly from the predicted λ^2 behavior. Closure amplitudes are quantities formed by combining the complex amplitudes in the correlated data ("visibilities") measured between sets of four different telescopes such that telescope-based gain errors cancel. The closure amplitude then provides a robust measure of the source size. Bower et al. attributed the deviations from the scattering law to the contribution of the intrinsic size, which was found to decrease with frequency. Measurements at higher frequencies by Shen et al. and Doeleman et al. [63, 64] confirmed this trend, revealing that indeed at 230 GHz ($\lambda = 1.3$ mm) the size is only 4 R_{S}. Fitting all data [61] one finds an intrinsic size of Sgr A* of

$$\phi_{\text{Sgr A}*} = (0.52 \pm 0.03)\,\text{mas} \times (\lambda/\text{cm})^{1.3\pm0.1}\,. \tag{2}$$

For the parameters used here (0.52 ± 0.03) mas correspond to $(51 \pm 3)\,R_{\text{s}}$ (see Figure 3, right).

2.4. Radio variability of Sgr A*

The radio emission itself is highly variable: rms variations of the radio spectrum are 2.5%, 6%, 16%, 17%, and 21% at wavelengths of 13, 3.6, 2, 1.3, and 0.7 cm respectively [61]. Hence, variability seems to increase in amplitude with increasing frequency. This is consistent with adiabatic expansion of plasma blobs flowing outwards (in a jet or otherwise) [65, 66]. At the highest frequencies [67, 68, 69, 70] one sees even larger rms variations with outbursts of a factor of several over the quiescent level.

Most interestingly, there seems to be a time lag between flares at different frequencies: 43 GHz flares precede 22 GHz flares by about 20 min [71]. Given that the
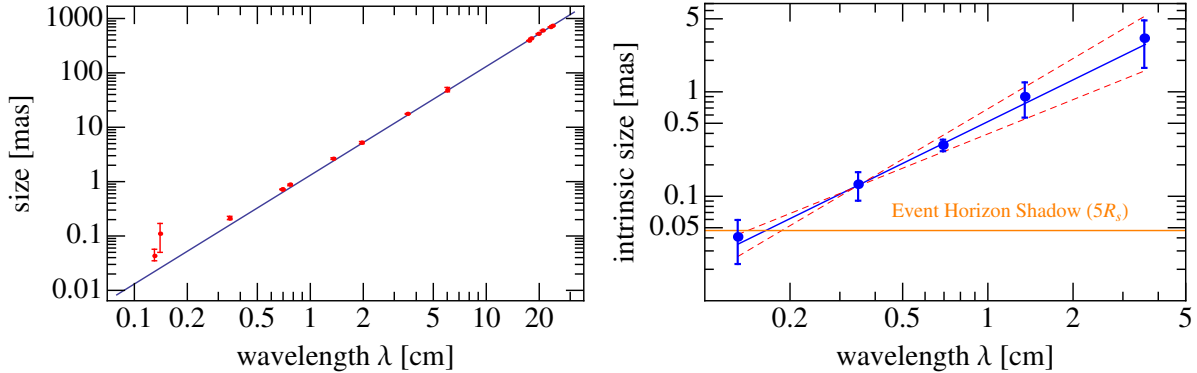
Figure 3 Left: measured major axis size of Sgr A* as function of wavelength measured by various VLBI experiments, the solid line indicates the λ^2 scattering law. Right: Derived intrinsic size of Sgr A* after subtraction of the scattering law using all available VLBI data (see [61] for details). The dashed line indicates the systematic uncertainties due to different normalizations of the scattering law, the predicted event horizon size due to lensing effects is indicated [13]. Figure taken from [4].

intrinsic size differences between these frequencies is about 30 light minutes, it would require relativistic outflows to propagate the flare from higher to lower frequencies, if they represent density or energy enhancements in the radio-emitting plasma [61]. Note that [71] interpret the lags as highly sub-relativistic outflows, based on a further claimed NIR-radio lag and not considering the size constraints.

2.5. Accretion boundary conditions: radio polarization and X-rays

Aside from the mass, the accretion rate onto the black hole is the second most important parameter, as it determines the level of activity and can vary by many orders of magnitude. Typically the radiated power of a luminous black hole can be used to infer the accretion rate, however this association becomes less linear for radiatively inefficient accretion flows (RIAFs). Initial estimates for the accretion rate onto Sgr A* ranged from $\sim 10^{-4} M_\odot/\text{yr}$ [72] to $10^{-6} M_\odot/\text{yr}$ [73], if Sgr A* is accreting from the winds of surrounding stars [74]. In the idealized case of Bondi-Hoyle accretion [75], the radial scale from which the BH can accrete (i.e., the Bondi radius R_B) depends only on the mass and speed of the surrounding gas, $R_\text{B} = 2GM/v_\text{w}^2$. For the stellar wind flow, early estimates of $v_\text{W} \sim 600 \text{ km s}^{-1}$ predicted $R_\text{B} \simeq 2.5 \times 10^5 R_\text{S} \simeq 0.1$ pc, corresponding to $\sim 2.5''$ projected on the sky in the Galactic Center ([76], scaled to today's value of the mass). From this radius inwards, the captured material is either entirely retained or mass can be lost via a variety of processes such as convection and/or winds [77, 78].

The best constraints we currently have on the accretion rate at the inner boundary near the black hole come from radio polarization measurements, because the polarization angle changes as it passes through a hot, magnetized medium. The polarization vector

rotates as $\Delta\phi = \mathrm{RM} \times \lambda^2$, where $\mathrm{RM} = 8 \times 10^5\,\mathrm{rad\,m^{-2}}\,\int B(s)\,n(s)\,\mathrm{d}s$ is the rotation measure, B is the line-of-sight magnetic field, n the free-electron density, and s the path length along the line-of-sight through the medium.

Bower et al. [79, 80] found that Sgr A* is essentially unpolarized between 5-43 GHz, which is quite different from what is found in quasars. They argued that the accretion flow itself could lead to a depolarization of the radiation by providing a very high RM, resulting in extremely fast rotation of the polarization vector.

This idea was corroborated by the detection of circular polarization [81], which usually is much lower than linear. Circular polarization is not affected by Faraday rotation and created by a related process, called conversion (see [82] for an explanation of both processes). The observed circular polarization has also maintained the same polarity for more than three decades [83, 84]. The interpretation is that of significant Faraday depolarization by thermal electrons in the source and a stable sense of rotation and polarity in the magnetic field structure producing the radiation [85, 82, 86, 87, 88].

The detection of strong linear polarization at (sub)mm-waves soon confirmed this picture [89, 90]. Indeed, the detected rotation measure of $RM \simeq -6 \times 10^5$ rad m^{-2} [91, 92, 93, 94] is the highest ever found in any source. By assuming a range of density and magnetic field profiles for accretion flows, the accretion rate can be constrained to lie between $\dot{M} \gtrsim 10^{-9} M_\odot/\mathrm{yr}$ and $\dot{M} \lesssim 10^{-7} M_\odot/\mathrm{yr}$ on scales of some hundreds to thousands R_s [85, 92, 92, 95, 88].

Around the time of the first polarization measurements, the *Chandra X-ray Observatory* was launched, with a spatial resolution of ~ 0.5". It discovered hot, thermal X-ray emission associated with Sgr A* with $k_\mathrm{B}T = 1.9$ keV, and resolved it to be slightly extended as one might expect for the bound accretion flow at $\sim R_\mathrm{B}$ [40]. Hence, this is likely the gas that Sgr A* is accreting from. For a sound speed

$$c_\mathrm{s} = \sqrt{\frac{5}{3}k_\mathrm{B}T/m_\mathrm{p}} = 550\,\mathrm{km/s}\,(k_\mathrm{B}T/1.9\,\mathrm{keV})^{1/2} \tag{3}$$

one finds again a Bondi accretion rate of

$$\dot{M}_\mathrm{Bondi} = 4\pi\,n\,G^2 M_\mathrm{bh}^2 c_\mathrm{s}^{-3} \tag{4}$$

$$\simeq 10^{-4}\,M_\odot\,\mathrm{yr}^{-1}\,\left(\frac{M_\mathrm{bh}}{4.3 \times 10^6 M_\odot}\right)^2 \left(\frac{n}{160\,\mathrm{cm^{-3}}}\right)\left(\frac{k_\mathrm{B}T}{1.9\,\mathrm{keV}}\right)^{-3}, \tag{5}$$

where the density normalization is based on what is inferred from X-ray measurements [40, 58]. The discrepancy with the much lower rate nearer the black hole implied from the radio polarization favors accretion scenarios which include mass loss associated with the inflow (see also [96]).

Most recently, a radio pulsar was found near Sgr A* [58, 97] at a projected distance of 0.1 pc, which also shows a very high RM of 7×10^4 rad m^{-2}, thereby requiring a few mG magnetic fields. This result not only supports the idea of the Faraday screen being locally associated with Sgr A*, but also suggests that the accretion flow is already starting with a high magnetization close to or even above the equipartition value [58].

2.6. Accretion boundary conditions: the G2 event

Finally, the discovery of an object coined "G2", by Gillessen et al. [98] heading for a close encounter with the BH, may soon provide an interesting opportunity to study basic accretion physics. G2 was discovered as an extended object emitting Brγ emission in a highly elliptical orbit around Sgr A*, which could be traced back to 2004. Recent observations [99] have confirmed the original finding: the object remains on track with a slightly later prediction for pericenter passage in spring of 2014 at a nominal pericenter distance of only 2200 Schwarzschild radii (R_s). The object's compact head shows a velocity shear of 600 km/s followed by a tail stretched over 400 mas.

The exact nature and origin of the object is still highly debated. The source could be a tenuous cloud as suggested by [98] or the disrupted atmosphere around a bound object like a star (e.g., [11]). Given the large shear much of the gas is already largely unbound even if the cloud would contain a star. Simulations [100, 101] predict that G2 will be disrupted and partially circularize at some thousand R_s, providing an average feeding rate above $\sim 10^{-7} M_\odot/\mathrm{yr}$. If that is true the properties of Sgr A* may change soon. On the other hand, the magnitude of the effect depends still on many unknown parameters and the current accretion rate onto Sgr A*. For example: how much mass is going to accrete and over which time scale? The actual free-fall time scale from $\sim$2000 R_s is roughly one month and the viscous time scale could be anywhere between months up to hundred years depending on the viscosity parameter α. The latter would dilute the effect considerably. At the time of writing, no discernable effect of the cloud has been observed.

2.7. Flares and variability, multi-wavelength data

Although Sgr A* has been known and characterized in the radio bands for decades, it proved rather elusive in other frequencies. Only after the launch of *Chandra* in 1999 was Sgr A* finally identified as a surprisingly weak X-ray source [40]. During the discovery observation, the first of what would turn out to be roughly daily X-ray flares was also detected [102]. The $\sim$hour long timescale for flare rise and decay provides a limit on the size scale of the emitting region, using light-crossing arguments without relativistic beaming, and corresponds to $\lesssim 10R_\mathrm{S}$. A few years later, once adaptive optics allowed for the further discovery of Sgr A* in the NIR, flares were also found in this band (e.g., [103, 43]). In the last decade of monitoring (see, e.g., [104],[45], and references in [10]) a picture has arisen where the steady, broadband radio and X-ray emission originates from larger scales while the more variable submm bump and NIR emission, as well as the X-ray flares, stem from non-thermal processes in the plasma very close to the black hole itself. Every X-ray flare seems to have a simultaneous NIR counterpart, but the reverse is not the case because smaller NIR flares may correlate with weak X-ray flares that cannot overcome the "blanket" of steady, thermal X-ray emission from larger scales. The submm-wave emission appears to be variable on somewhat longer timescales [69] and may not correlate as strongly – or at all – with the NIR/X-ray variability, likely

because of optical depth effects.

Until recently, the general picture developed that Sgr A*'s spectrum could be divided into "quiescent" and "flaring" states, based on the apparent dichotomy of X-ray behavior and NIR flare analyses (e.g., [45]). However, a reanalysis suggests that the NIR flares may be consistent with a single [105] power-law flux distribution, meaning that Sgr A* is likely continually variable down to weak flares that are indistinguishable from an average, lowest state which one could associate with "quiescence". The interpretation of the flares is an area of active debate.

The largest multi-wavelength campaign on Sgr A* was recently conducted using *Chandra* as part of the X-ray Visionary Project (XVP) class‖. These 35 days of observations within one year roughly doubled the photon count compared to the prior 12 years, and tripled the number of detected X-ray flares, allowing the first statistical tests to be performed similar to the NIR studies. These observations also utilized the High Energy Transmission Gratings Spectrometer (HETGS; [106]) for the first time, providing high-resolution spectroscopy in addition to the highest spatial resolution available in the X-ray band. As part of this effort, an extensive network of ground and space-based observatories were deployed, to obtain (quasi)-simultaneous data from the radio through TeV γ-ray frequencies. In the next section, after introducing the theoretical context, we will briefly summarize the latest conclusions from these campaigns.

3. Models

3.1. Accretion models

Because Sgr A* is the closest SMBH to us, its value as a testbed for accretion theory has led to very active debates about the exact nature of its emission processes and physical geometry. Each particular model for the emission can lead to radically different interpretations of the data near the black hole, and impact on our ability to tease out information about strong gravity effects, thus properly understanding the astrophysics is a key "foreground" to the gravitational scenarios.

By now it is generally accepted that all massive galaxies contain a supermassive black hole, but Sgr A*'s extremely low level of activity has provided several puzzles. First of all, the current accretion rate is about four orders of magnitude below the average accretion rate needed to grow a few million solar mass in a Hubble time. Secondly, the radio luminosity of Sgr A* seems to be well below the break in the luminosity function for radio cores [107] in low-luminosity AGN and hence marks a rather low state in the activity level of SMBHs in galaxies¶, and thirdly the amount of gas available to fuel the black hole would imply emission many orders of magnitude larger than what is observed (i.e., comparing $\sim 10\% \, \dot{M}_{\mathrm{Bondi}} c^2 = 6 \times 10^{41}$ erg/sec to $\nu L_\nu(350\,\mathrm{GHz}) \sim 10^{35}$ erg/sec [109]).

‖ Sgr A* XVP website: `http://www.sgra-star.com/`
¶ There have even been anthropic arguments on why the activity level in our Galaxy is so low [108].

The extremely weak radio and X-ray emission ($L(2 - 10\,\mathrm{keV}) \sim 2.5 \times 10^{33}$ erg/sec) led to a renaissance of RIAF models, starting with the so-called advection-dominated accretion flow (ADAF; [110, 111]) as well as others (e.g., [76, 78, 77]). These models share a common theme of reducing the radiative efficiency via either "hiding" the energy in less radiative protons and ions that advect it beyond the event horizon, or in also allowing mass loss from the accretion flow via convection and/or outflows. Because more heat is retained, the disk puffs up from gas pressure while at the same time becoming optically thin and radiatively inefficient because of the low particle densities. This low luminosity is somewhat more of a blessing than a curse because radiation effects on the dynamics can be ignored — in marked contrast to the accretion disks of quasars, that require one to include much more physics.

The original models for Sgr A* were so inefficient that they required much higher accretion rates, but these were adapted after the new radio polarization results became available that reduced the accretion rate considerably (see section 2.5). Interestingly the one model which did not have to be changed was the one attributing the emission to a jet (see below), which already required low accretion rates from the innermost scales because it is in fact relatively radiatively efficient [112, 113].

An important caveat in all these models is the unknown heating mechanism of electrons via some form of weak coupling to the protons/ions. This missing element of the microphysics has allowed tuning the radiative efficiencies to a wide range of accretion rates and remains a major source of uncertainty. Hence, the exact value of $\dot{M}$ is still model-dependent. Recent studies of the accretion flow using sophisticated three-dimensional general relativistic hydrodynamic (3D GRMHD) simulations require values at the lower end of the range to reproduce the submm-wave spectrum [114, 88, 115, 116] from the accretion flow (but ignoring a jet contribution). The latter two works in particular utilize the first GRMHD code to include radiative cooling self-consistently, and to fit the submm bump they also favor an accretion rate of a few $10^{-9} M_\odot/\mathrm{yr}$.

In any case, it seems that only a tiny fraction of the captured material actually makes it down to the inner regions near the black hole, while the rest is seemingly lost. The newest results from the XVP campaign provide the most direct evidence yet for such an outflow, as well as for the source of fuel at the outer boundary. As described in [96], the diffuse emission is now resolved to be elongated in a direction consistent with the stellar disk observed in the NIR, strongly supporting the stellar-feeding paradigm. Furthermore, the use of the HETGS for the first time allowed the resolution of the Fe K_α complex into distinct lines. The measured ratio of H-like to He-like Fe lines allows the radial profile of the gas temperature and density to be constrained. The results effectively rule out the "no outflow" scenario and further support the various branches of "lossy" RIAF solutions (i.e., decreasing $\dot{M}$ as function of radius), as well as earlier estimates of the radial profile by [117]. These powerful new constraints will need to be convolved into the models of emission profiles, polarization, and eventually GR effects as described in the following section.

3.2. Contributions from a jet in Sgr A*

Another major puzzle is whether Sgr A* is launching collimated jets of relativistic plasma, as is the norm in other known weakly accreting black holes. Already over 30 years ago, [118] suggested an origin of the radio emission in a jet or wind (but from a stellar-sized object). Indeed, the properties of Sgr A* resemble those of flat/inverted-spectrum compact radio cores in more luminous AGN (later also found in X-ray binaries), which can be explained as the superposition of $\tau{=}1$ surfaces (the photosphere, where optical depth becomes unity) in a stratified relativistic jet. From conservation laws, larger scales correspond to less dense regions with lower magnetic fields, and thus lower frequency emission (see, e.g., [119]).

This issue was later revisited where the observed spectrum and frequency-dependent size of Sgr A* was explained as a scaled-down quasar jet from an "AGN on a starvation diet", i.e., a supermassive black hole with very low accretion rate [112, 113]. Based on the "jet-disk symbiosis assumption" [120], where the total jet power simply is $Q_{\mathrm{jet}} = q_{\mathrm{j}}\dot{M}_{\mathrm{disk}}$ and $q_{\mathrm{j}} \sim 3-10\%$, a number of concrete predictions were made [121, 113, 122] that have consistently been borne out by observations, such as the frequency-dependent size of Sgr A* [62] or radio outbursts that travel from high to low frequencies, i.e., from the inside-out, with relativistic speeds [123].

These results are also consistent with semi-analytical (e.g., [124]) and GRMHD simulations (e.g., [125, 126]) that favor geometrically thick accretion flows with ordered magnetic fields as preferential launch sites for relativistic jets. Indeed, it was recently shown [127] that the jets produced in such simulations can fully reproduce the observed flat-to-inverted radio spectrum when reasonable particle acceleration processes are considered. Thus we finally have full GRMHD simulations that can reproduce inflow and outflows as well as the overall spectrum and size of Sgr A*..

However, jets have not yet been directly imaged emanating from Sgr A* (though see [128]), and although arguments can be made about why intervening scattering can easily hide jets [129], alternate models have been proposed in which the radio emission is produced in the accretion flow itself (e.g., [130]). On the other hand, the radio time lags discussed in section 2.4 suggest a relativistic outflow and Sgr A*'s non-thermal emission during bright X-ray flares fits on the "fundamental plane of black hole activity". The fundamental plane connects radio- and X-ray emission of all types of weakly accreting black holes as a function of black hole mass [131, 132]. This includes stellar mass black holes at almost the same level of quiescence [133, 134] as Sgr A*. Thus it seems likely that Sgr A* is underfed, radiatively inefficient, and launching a jet (e.g., [135]).

3.3. Flares and particle heating

So far we have been discussing the steady emission, but the NIR/X-ray flares have provided a third major puzzle, and an opportunity to probe directly the plasma conditions very close to the black hole (within tens of R_{S}). The fast timescale of the flares, simultaneous NIR variability, and the flattening of the X-ray spectrum all argue

for a non-thermal process. Most groups to date have generally focused on magnetic processes similar to those in the solar corona, where magnetic reconnection or stochastic processes can provide fast heating and particle acceleration [122, 136, 137], resulting in either direct synchrotron emission in the X-ray band, or synchrotron-self Compton (SSC) emission from the up-scattered submm-bump photons. However, a population of asteroids fragmented and vaporized within Sgr A*'s accretion flow can also instigate NIR/X-ray flares consistent with the observations [138]. Distinguishing between models requires strictly simultaneous data, which is challenging to obtain. The simultaneity of at least some flares in NIR and X-ray, e.g., [139] favors the SSC interpretation, while others favor direct synchrotron [140], and it is not unlikely that there is an interplay between both processes.

An interesting effect of particle acceleration during NIR/X-ray flares could be an increase in the intrinsic size of the jet photosphere. The size of the photosphere is strongly dependent on the radiating particle distribution, and the predominantly thermal distribution required by the submm bump allows for a small size even in jet models (see, e.g., [129]). If, however, a bright flare results from sustained particle acceleration and that plasma is then advected into the jet, one might be able to detect variability in the measured size associated with NIR/X-ray flares. Within the context of the XVP-linked multi-wavelength coordinated campaign, VLBA observations were triggered from NIR flares, and the first hint of variability in the radio photosphere size was observed [141] (see also [70]).

Another exciting highlight of the XVP campaign is the detection of enough new X-ray flares with high enough cadence to study their statistical properties. These recent results are summarized in [41], where a variability analysis of the flares provides clues about the innermost orbit of accreting plasma and thus indirectly constrains the event horizon scale. The results are still preliminary but suggest a cutoff timescale for flares on the order of the light-crossing time of the innermost stable circular orbit (ISCO) and a variability component in the power density spectrum above Poisson noise that is consistent with the same timescale. Such quasi-periodic oscillations (QPOs) have been predicted in some accretion models of the flow from magnetic processes [142, 143] or Lense-Thirring precession [144] near the ISCO, with various claimed detections in the past in X-ray [145] and NIR [146] that have, however, not been robust against statistical analysis [104]. Thus although still very controversial, the prospect of QPOs from Sgr A* is tantalizing because they may offer another potential route (see, e.g., [147]) to study GR effects in addition to imaging.

4. Observable general relativistic effects

4.1. The shadow

The presence of radiation so close to the event horizon and the availability of a suitable observing technique, namely VLBI, begs the question of what the observable effects of

general relativity on the image are?

The visual appearance of a black hole is a question that already received attention rather early on. For example, Bardeen [148] calculated the shape of a star behind a black hole. While this situation is exceedingly unlikely and the effect is too small to be observable in practice, it provided important clues on what to expect (see Figure 4 in [121] and Fig. 4 for more recent similar examples). With the emerging idea of optically thick, geometrically thin accretion disks [149] surrounding and illuminating black holes, Cunningham calculated such a scenario with a focus on how the spectrum would be modified by gravitational redshift and lensing [150]. Hollywood & Melia applied this framework to the infrared spectrum of Sgr A* [151] for a Bondi-Holye disk and Viergutz [152] calculated general images of accretion disks. Typically these disks were truncated near the innermost circular orbit (ISCO) of matter, and hence the main effect is the deformation of a ring the size of the ISCO by gravitational light bending near the black hole, rather than the effect of the event horizon itself.

When the relevance of the submm bump in Sgr A* was realized, Falcke, Melia, & Agol [13, 121], building on the work of Bardeen, calculated the appearance of a black hole surrounded by an optically thin emission region on (sub-)ISCO scales, as is likely the case in Sgr A*. They identified what they called the "shadow of the black hole" as a tell-tale feature of the event horizon superimposed over the background light, which could be reasonably detected with (sub)mm-wave very long baseline interferometry (VLBI) in Sgr A*[+].

The shadow is essentially a lensed image of the event horizon and its shape is closely related to the photon orbit, which describes a closed orbit for photons around the black hole. Since photons that circle the black hole slightly within the photon orbit will end up inside the event horizon while photons just outside will escape to infinity, there is a rather sharp boundary between bright and dark regions. The shadow itself is thus indeed primarily a deficit of photons due to absorption by the event horizon. Given that light rays circling outside the photon orbit pass longer through light-emitting material (if optically thin), there is also a possibility of an enhanced photon ring surrounding the shadow [154, 155].

The diameter of the shadow is only marginally dependent on spin, ranging from $4.5\,R_\mathrm{s}$ for a maximally spinning black hole to $\sqrt{27}\,R_\mathrm{s}$ for a Schwarzschild black hole. This is in marked contrast to other properties of black holes, such as the ISCO, which strongly scales with spin. Light rays passing on the side where they are co-rotating with the black hole come much closer to the center of mass with increasing spin than light rays passing on the other, i.e., counter-rotating, side. The latter have to pass at much larger distances to avoid being caught in the event horizon. Hence, the centroid of the shadow can shift significantly with respect to the mass center, but shrinks only by some $\sim 10\%$ as a function of spin.

Given that the black hole location in an image is difficult to measure, the shift

[+] The same term was independently introduced also by de Vries [153] in a more mathematical treatment of the problem and again applied to optical observations of more distant black holes.

itself may be hard to detect. Nonetheless, the spin still has a marked impact on the appearance [156, 157, 158]. For one, the higher the spin, the closer the photon orbit and the higher the emissivity on the co-rotating side. Secondly, the relativistic beaming effect due to the emitting material (if co-rotating with the black hole spin!) will amplify the co-rotating side further and a spinning black hole will have a much stronger asymmetry compared to a non-rotating black hole. The effect of spin is also dramatic in terms of the spectral properties of the submm bump [114, 116].

4.2. Testing theories of gravitation

In the meantime an entire "shadow industry" has emerged that proposes to test general relativistic effects using imaging techniques.

First of all, the detection of the shadow would distinguish between objects with and without an event horizon [159]. There are reasonable arguments based on the emitted spectrum alone that an event horizon should exist in Sgr A* [53, 160, 161], but "seeing is believing" in science.

Secondly, one could start to test alternatives to standard Kerr black holes, such as super-spinning black holes [162], boson stars [163], gravastars [164], wormholes [165], and massless braneworld black holes [166]. In boson stars, for example, the shadow is expected to be less sharp and super-spinning black holes have a much smaller shadow — if any. In addition, of course, one always needs to verify that any alternative model can also address the full range of astrophysical properties observed in Sgr A* and other black hole candidates. For example, if a specific boson mass is required, it should probably not vary between different galaxies.

Moreover, it has also been suggested that non-standard GR theories could be tested or at least constrained, such as Kerr-Taub-NUT black holes [167], charged Reissner-Nordström black holes [168], rotating Hořava-Lifshitz black holes [169], Sen black holes [170], Kaluza-Klein rotation dilaton black holes[171], black holes in $\delta = 2$ Tomimatsu-Sato (TS2) spacetime [172], and in general black holes in space times with extra dimensions [173]. It has also been pointed out that one can use the Sgr A* shadow to distinguish a Kerr hole from a naked singularity [158] and of course from the combination of multiple black holes [174]. The latter, however, seems very unlikely in the Galactic Center due to the positional stability of the radio source [175].

Johannsen & Psaltis [154] chose a slightly different approach by allowing for a small perturbation to the quadrupole moment (besides spin and mass) of a black hole and calculating the images in the corresponding metric. While not born by any theory of gravity this allows one to quantify the validity of the no-hair theorem.

Many of these studies are not yet quantitative enough that it is easy to tell how well an actual observation of Sgr A* can distinguish one model from the other in the presence of instrumental limitations. Figure 4 shows a sample of different contours of black hole shadows in different metrics. Indeed, certain spacetimes, like Kaluza-Klein black holes, can produce strong changes that should be readily distinguishable, while
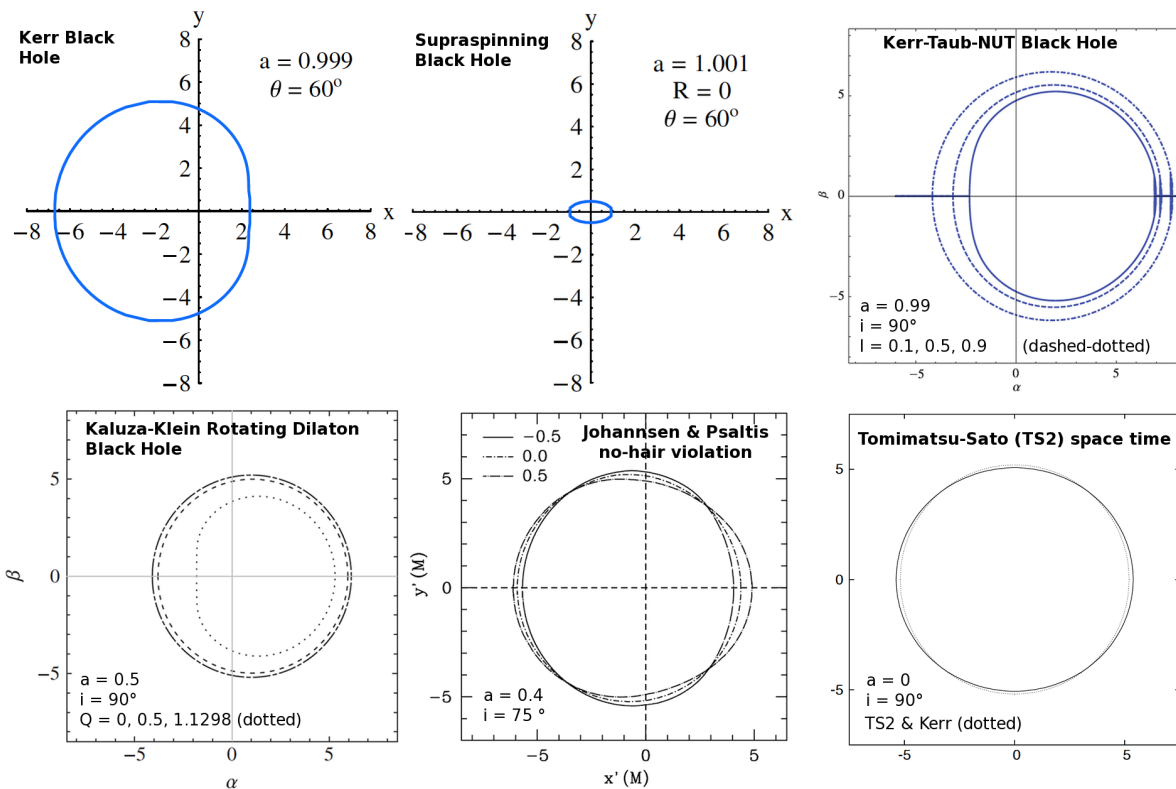
Figure 4   Collection of shadow contours for different types of (non-standard) black holes. From top-left to bottom right: Kerr black hole (as reference), super-spinning black hole [162], Kerr-Taub-NUT black hole [167], Kaluza-Klein rotation dilaton black holes [171], a parametrized no-hair violation black hole [154], black holes in Tomimatsu-Sato spacetime [172]. The relevant parameters as used in the respective papers are given in the panels. If multiple lines are plotted and multiple parameters are listed, then the line type corresponding to the last parameter value is also given. Note that Johannsen & Psaltis plot the contours of the photon ring surrounding the shadow rather than the shadow itself.

others, like TS2 spacetime, only produce a few-percent wobbles on the shadow, which would require extremely precise measurements. This plethora of scenarios probably warrants a meta-study to convolve all these predictions with actual detector simulations, similar to those trying to constrain spin and inclination from current data based on the Kerr metric [176].

4.3. The role of astrophysical models

An important caveat is certainly the unknown structure of the astrophysical source of emission. The fact that the emission becomes optically thin in the submm-wave regime is well established by the turnover in the submm bump as well as the change in polarization. In the transition region however, which will be observed in the first experiments at 230 GHz, optical depth effects can still be expected to play a role and

will be somewhat model dependent. Similarly, while the existence of a shadow itself is generic to all models, its detailed appearance and brightness distribution will depend strongly on the underlying astrophysical model as discussed in section 3. Hence, black hole parameter estimates from simulations are premature. The reason why this is a difficult issue, is that the visual appearance is not only determined by the structure of the plasma flow alone, but also by the assumed heating and acceleration of electrons — a microphysical process that is not well understood yet. One might think that electrons are just the icing on the cake, but if the icing is the only thing one can see, the actual shape of the cake can quickly become a secondary factor.

Nonetheless, many shadow images have been calculated using MHD models [177, 178, 114, 179, 176, 4] and compared to VLBI data (real or simulated) and provided reasonable agreement. The most dramatic change in expected emission properties is seen when taking potential emission from the jet into account [127]. However, even in this case the shadow structure is still discernable at 230 GHz. In addition, polarization of the emission and its signatures while passing near the black hole can provide additional information [180, 181, 182], even though calculating polarized radiation transport in an ionized medium near a black hole is far from trivial [183].

4.4. The experimental side

The shadow itself remains a rather robust feature of these simulations unless the optical depth becomes large. Figure 5 shows one example. If the orientation and spin are favorable, the shadow should be easily visible. However, if the orientation is more edge-on and the spin is high, the contrast between approaching and receding ring will be high as well.

Indeed, under the assumption that the emission is described by a simple RIAF model, Broderick et al. [184] argue that face-on models are already highly disfavored by current data. After all, some basic information about orientation and basic structure can already be retrieved by just combining three telescopes to measure the closure phase[*] at 230 GHz, which turns out to be quite constraining in ruling out various models [176]. VLBI simulations with a larger array of (existing) telescopes have been published in [185, 186], but given the systematic uncertainty in predicting the correct astrophysical model, there is no clear understanding yet how reliably black hole parameters such as spin can be determined.

Clearly, three baselines will not be sufficient to convincingly measure a shadow. In particular, the edge-on example of Fig. 5 requires much higher dynamic range in the imaging ($>200{:}1$) and hence a sizable number of sensitive telescopes ($\gtrsim 6-10$) [4]. Given that interferometry is very precise in measuring sizes, and the astrometric precision increases linearly with signal-to-noise, it does not seem unreasonable that deviations of $\lesssim 10\%$ from the expected shape could be detectable with current technology. A

---

[*] In contrast to the closure amplitude, which is sensitive to the source size, the closure phase is very sensitive to the source structure.
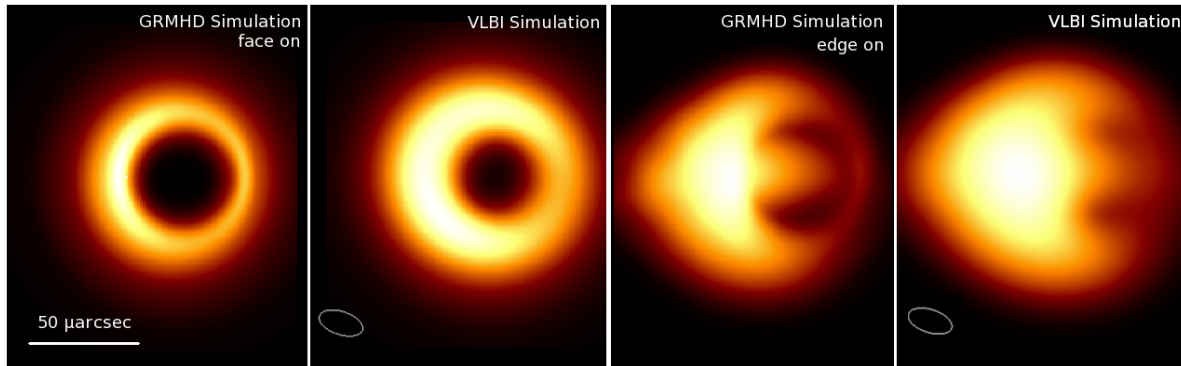
Figure 5 GRMHD simulation [114] of the emission in an accretion flow around a rapidly spinning BH in Sgr A* blurred according to the expected interstellar scattering. This is compared to a reconstructed image from simulated submm-VLBI for face-on and edge-on orientations of the accretion flow [4]. The small white ellipse indicates the reconstructed beams sizes. In the optimal case (face-on), the shadow is easily visible, while in the most pessimistic case (edge-on) a dynamic range $\gtrsim$200:1 is needed to reveal the faint photon ring.

dedicated array built for just this purpose might, however, do even better in the future — especially if higher frequencies (>350 GHz) can be utilized, perhaps even from space.

At present one has to be content with existing submm-wave telescopes, though major breakthroughs have already been achieved at frequencies of $\sim$ 230 GHz [187, 64, 188], where interferometry is still in its experimental phase. Nonetheless, around the world, groups are gearing up to combine the available submm-wave telescopes into an "Event Horizon Telescope", which would provide the highest resolution "camera" available in astrophysics [189, 190, 191]. A crucial element of this plan will be the Atacama Large Millimetre Array (ALMA) which provides unprecedented sensitivity if properly equipped for VLBI.

It is very important to remember that not every interferometer nor any wavelength will do: the emission must be produced at event horizon scales and must also be optically thin! For Sgr A* we know this to be true only in the submm-wave, IR and X-ray regimes, but only submm has the potential currently for global interferometry. Also, should the accretion rate increase substantially, e.g., due to something like the G2 event, the source could become optically thick even at submm-waves and, e.g., far-infrared interferometry would be needed.

Apart from the Galactic Center the nearby elliptical galaxy M87, with its powerful radio jet, may also lend itself to observing a black hole shadow. Other black holes are too small at their respective distances [14] and would require very novel and difficult techniques, such as X-ray interferometers [192], which are far from likely in the current funding environment.

4.5. More than a shadow: stars and pulsars

Finally, it is not imaging alone that promises significant advances in testing general relativity in the Galactic Center. The NIR field will advance further using interferometry together with a technique called phase-referencing, allowing very high positional accuracy for very faint objects. For instance, ESO's planned GRAVITY instrument [193] should be able to detect stars orbiting the black hole at even tighter orbits, and provide astrometry at the 10μas level, thereby providing even better mass measurements. The general-relativistic periastron shift and the Lense-Thirring precession of the orbital angular momentum will influence such stellar orbits and, for stars passing at small distances from the BH, the timescale of these relativistic effects is short enough to be within the reach of GRAVITY, thus allowing one to constrain the BH spin from stellar orbits.

Since the imaging resolution of IR interferometry using the VLT is on the milliarcsecond level, the shadow itself cannot be resolved. However, it has been suggested that the effect of orbiting hotspots around the black hole could lead to detectable position shifts, polarization variation, and position-intensity correlation that are expected for a source orbiting a black hole.

Another real breakthrough would be the discovery of a pulsar orbiting Sgr A* on a tight orbit. In principle, it is already sufficient to find and time a single normal, slowly rotating pulsar in an orbit similar to that of stars targeted by GRAVITY, to measure the mass of Sgr A* with a precision of 1 solar mass, i.e., a relative precision of $< 10^{-6}$. Such a pulsar could in principle also determine the black hole spin to 0.1%, and the quadrupole moment, testing the no-hair theorem, to 1% [194, 195]. In general, a stellar mass pulsar in orbit around a supermassive black hole, will probe a completely new parameter space in relativity. Alas, until recently not a single pulsar had been found within some ten parsecs of the Galactic Center, despite the expectation to see thousands [196]. Finding a pulsar in the Galactic Center is perhaps one of the most difficult challenges in pulsar astronomy, due to the strong acceleration of the source and dispersion and scattering of the signal. Fortunately, there is some hope as the first radio pulsar within 0.1 pc of Sgr A* has just been found [58, 97]. With sensitive telescopes such as the VLA and ALMA, the big single dishes (Parkes, Effelsberg, GBT), and the SKA in the future, more advanced searches may turn up many more of these.

5. Summary and conclusion

The good news is that there is a very strong case for a supermassive black hole in the center of our Milky Way whose event horizon can be imaged with radio interferometry techniques. In Table 1 we summarize its main properties reviewed here. The mass of the black hole is robustly determined from stellar orbits — better than for any other black hole candidate in the universe and confirmed by different groups and different telescopes. The mass is also clearly associated with a compact radio source, Sgr A*,

that is physically located in the Galactic Center and which does not show any motion itself — as expected for a massive object. The accretion rate onto the black hole is constrained in both directions by radio polarization observations and X-ray imaging. Sgr A*'s low bolometric luminosity as well as its spectrum cutting off in the submm-wave (THz) regime supports the presence of an event horizon. Radio interferometry measurements confirm that the radio emitting region becomes smaller as the frequency increases and that it approaches event horizon scales at frequencies above 230 GHz. A spectral turn-over at these frequencies indicates that the region transitions to become optically thin and allows us to see through to the event horizon. This effect should lead to the appearance of a "black hole shadow", which is a lensed image of photons absorbed into the event horizon. The shadow is in principle detectable with present-day technology and would allow many fundamental tests of general relativity and its alternatives.

Combining the information from submm-wave interferometry, broadband multi-wavelength observations, stellar orbits, potentially the information from pulsars, and coupled to advanced general relativistic and magnetohydrodynamic simulations will provide us with an outstanding astrophysical laboratory – likely the best there is and ever will be – of general relativity in its strongest limit and of black hole astrophysics.

If we ever want to know whether the dark objects lurking in the centers of galaxies are really supermassive black holes and want to understand how they work, the Galactic Center is the place to study. The nearby galaxy M87 may corroborate these results in the future, but it will always suffer from a lower confidence in independent mass determinations and hence can only supplement studies of Sgr A*.

Together with gravitational wave detections of merging black holes and the detection of a pulsar-black hole binary, the Galactic Center therefore promises a golden future for experimental studies of general relativity

Acknowledgments

References

[1] S. Boissier and N. Prantzos. Chemo-spectrophotometric evolution of spiral galaxies - I. The model and the Milky Way. MNRAS, 307:857–876, August 1999.

[2] M. Samland. Modeling the Evolution of Disk Galaxies. II. Yields of Massive Stars. ApJ, 496:155, March 1998.

Table 1 Sgr A* fact sheet

Property	Value	Ref.
Position (J2000)	$\alpha(1996.25) = 17^{\text{h}}45^{\text{m}}40\overset{\text{s}}{.}0409, \quad \delta(1996.25) = -29°00'28''118$	[33]
Position (Galactic)	$l(1996.25) = 359.9442085, \quad b(1996.25) = -0.04609407$	[33]
Proper motion (equatorial)	$\dot{\alpha}_{\text{east}} = -3.151 \pm 0.05$ mas yr^{-1}, $\quad \dot{\delta}_{\text{north}} = -5.547 \pm 0.13$ mas yr^{-1}	[34]
Proper motion (Galactic)	$\dot{l}_{\text{long}} = -6.379 \pm 0.13$ mas yr^{-1}, $\quad \dot{b}_{\text{lat}} = +0.202 \pm 0.02$ mas yr^{-1}	[34]
Mass	$M_{\text{Sgr A}*} = 4.3(\pm0.4) \times 10^6 M_\odot = 8.5(\pm0.8) \times 10^{36}$ kg	[26]
Distance	$D_{\text{Sgr A}*} = 8.35(\pm0.15)$ kpc $= 2.58(\pm0.05) \times 10^{17}$ km	[26][32]
Angular scales	1 mas $= 1.2 \times 10^9$ km $= 98\ R_s, \quad 1'' = 1.2 \times 10^{12}$ km $= 0.04$ pc $30'' = 4 \times 10^{13}$ km $= 1.2$ pc, $\quad 10' = 24$ pc	
Gravitational radius	$R_g = GM/c^2 = 6.3 \times 10^6$ km $\sim 5.1\ \mu$as	
Schwarzschild radius	$R_S = 2GM/c^2 = 13 \times 10^6$ km $\sim 10.2\ \mu$as	
ISCO for non-rot. BH	$R_{\text{ISCO}} = 6GM/c^2 = 3.8 \times 10^7$ km $\sim 30.7\ \mu$as	
Orbital timescale at ISCO	$\tau_{\text{orb}} \simeq 2\pi Sqrt{6^3}R_6/c = 65.2$ min $\left(M_{\text{bh}}/4.3 \times 10^6 M_\odot\right)$	[197, 198]
Shadow diameter (a=0)	$d_{\text{Shadow}} = \sqrt{27}\ R_s \simeq 53\ \mu$as	
Shadow diameter (a=1)	$d_{\text{Shadow}} = 9/2\ R_s \simeq 46\ \mu$as	
Measured size	$\phi_{\text{Sgr A}*} = (0.52 \pm 0.03)$ mas $\times (\lambda/\text{cm})^{1.3\pm0.1}$	[61]
	$R_{\text{Sgr A}*} = (51 \pm 3)\ R_s \times (\lambda/\text{cm})^{1.3\pm0.1}$	[61]
Rotation measure	$RM \simeq -6 \times 10^5$ rad m^{-2}	[93, 94]
Accretion rate ($R \lesssim 100 R_s$)	$10^{-7} M_\odot/\text{yr} \gtrsim \dot{M} \gtrsim 10^{-9} M_\odot/\text{yr}$	[92, 85]
Bondi radius	$r_{\text{Bondi}} = 2GM_{\text{bh}}/c_s^2 = 0.12$ pc $\left(M_{\text{bh}}/4.3 \times 10^6 M_\odot\right)(c_s/550\,\text{km/s})^{-2}$	
	$r_{\text{Bondi}} = 3 \times 10^5 R_s \sim 3''$	
Grav. sphere of influence	$R(M_{\text{BH}} = M_{\text{stars}}) \simeq 3$ pc	[26]
Eddington luminosity	$L_{\text{edd}} = 4\pi GM m_{\text{p}} c/\sigma_{\text{T}} = 5 \times 10^{44}\left(M_{\text{bh}}/4.3 \times 10^6 M_\odot\right)$ erg/sec	
Radio luminosity	$\nu L_\nu(350\,\text{GHz}) \sim 10^{35}$ erg/sec $\sim 2 \times 10^{-10} L_{\text{edd}}$	[109]
X-ray luminosity	$L(2-10\,\text{keV}) \sim 2.5 \times 10^{33}$ erg/sec $\sim 4.6 \times 10^{-12} L_{\text{edd}}$	[40]

[3] P. G. Jonker, C. G. Bassa, G. Nelemans, D. Steeghs, M. A. P. Torres, T. J. Maccarone, R. I. Hynes, S. Greiss, J. Clem, A. Dieball, V. J. Mikles, C. T. Britt, L. Gossen, A. C. Collazzi, R. Wijnands, J. J. M. In't Zand, M. Méndez, N. Rea, E. Kuulkers, E. M. Ratti, L. M. van Haaften, C. Heinke, F. Özel, P. J. Groot, and F. Verbunt. The Galactic Bulge Survey: Outline and X-ray Observations. ApJS, 194:18, June 2011.

[4] H. Falcke, S. Markoff, G. C. Bower, C. F. Gammie, M. Mocibrodzka, and D. Maitra. The jet in the galactic center: An ideal laboratory for magnetohydrodynamics and general relativity. In G. E. Romero, R. A. Sunyaev, and T. Belloni, editors, *IAU Symposium*, volume 275 of *IAU Symposium*, pages 68–76, February 2011.

[5] D. Lynden-Bell and M. J. Rees. On quasars, dust and the galactic centre. MNRAS, 152:461, 1971.

[6] B. Balick and R. L. Brown. Intense sub-arcsecond structure in the galactic center. ApJ, 194:265–270, December 1974.

[7] R. D. Ekers, W. M. Goss, U. J. Schwarz, D. Downes, and D. H. Rogstad. A full synthesis map of sgr a at 5ghz. A&A, 43:159–166, October 1975.

[8] R. Genzel and C. H. Townes. Physical conditions, dynamics, and mass distribution in the center of the galaxy. ARA&A, 25:377–423, 1987.

[9] F. Melia and H. Falcke. The Supermassive Black Hole at the Galactic Center. ARA&A, 39:309–352, 2001.

[10] R. Genzel, F. Eisenhauer, and S. Gillessen. The Galactic Center massive black hole and nuclear star cluster. *Reviews of Modern Physics*, 82:3121–3195, October 2010.

[11] M. R. Morris, L. Meyer, and A. M. Ghez. Galactic center research: manifestations of the central black hole. *Research in Astronomy and Astrophysics*, 12:995–1020, August 2012.

[12] H. Falcke and F. Hehl, editors. *The Galactic Black Hole*. Series in High Energy Physics, Cosmology and Gravitation. The Institute of Physics Publishing, Bristol, UK, December 2002.

[13] H. Falcke, F. Melia, and E. Agol. Viewing the shadow of the black hole at the galactic center. ApJ, 528:L13–L16, January 2000.

[14] T. Johannsen, D. Psaltis, S. Gillessen, D. P. Marrone, F. Özel, S. S. Doeleman, and V. L. Fish. Masses of nearby Supermassive Black Holes with Very Long Baseline Interferometry. ApJ, 758:30, October 2012.

[15] A. Blaauw, C. S. Gum, J. L. Pawsey, and G. Westerhout. The new I. A. U. system of galactic coordinates (1958 revision). MNRAS, 121:123, 1960.

[16] J. H. Lacy, C. H. Townes, T. R. Geballe, and D. J. Hollenbach. Observations of the motion and distribution of the ionized gas in the central parsec of the Galaxy. II. ApJ, 241:132–146, October 1980.

[17] E. Serabyn, J. H. Lacy, C. H. Townes, and R. Bharat. High-resolution forbidden NE II observations of the ionized filaments in the Galactic center. ApJ, 326:171–185, March 1988.

[18] D. A. Roberts and W. M. Goss. Multiconfiguration VLA H92-alpha observations of Sagittarius A West at 1 arcsecond resolution. ApJS, 86:133–152, May 1993.

[19] J.-H. Zhao, R. Blundell, J. M. Moran, D. Downes, K. F. Schuster, and D. P. Marrone. The High-density Ionized Gas in the Central Parsec of the Galaxy. ApJ, 723:1097–1109, November 2010.

[20] A. Eckart, R. Genzel, R. Hofmann, B. J. Sams, and L. E. Tacconi-Garman. Near-infrared 0.15 arcsec resolution imaging of the Galactic center. ApJ, 407:L77–L80, April 1993.

[21] A. Eckart and R. Genzel. Observations of stellar proper motions near the galactic centre. Nature, 383:415–417, 1996.

[22] A. M. Ghez, B. L. Klein, M. Morris, and E. E. Becklin. High proper-motion stars in the vicinity of sagittarius a*: Evidence for a supermassive black hole at the center of our galaxy. ApJ, 509:678–686, December 1998.

[23] A. M. Ghez, M. Morris, E. E. Becklin, A. Tanner, and T. Kremenek. The accelerations of stars orbiting the milky way's central black hole. Nature, 407:349–351, September 2000.

[24] R. Genzel, C. Pichon, A. Eckart, O. E. Gerhard, and T. Ott. Stellar dynamics in the Galactic Centre: proper motions and anisotropy. MNRAS, 317:348–374, September 2000.

[25] A. M. Ghez, S. Salim, N. N. Weinberg, J. R. Lu, T. Do, J. K. Dunn, K. Matthews, M. R. Morris, S. Yelda, E. E. Becklin, T. Kremenek, M. Milosavljevic, and J. Naiman. Measuring Distance and Properties of the Milky Way's Central Supermassive Black Hole with Stellar Orbits. ApJ, 689:1044–1062, December 2008.

[26] S. Gillessen, F. Eisenhauer, S. Trippe, T. Alexander, R. Genzel, F. Martins, and T. Ott. Monitoring Stellar Orbits Around the Massive Black Hole in the Galactic Center. ApJ, 692:1075–1109, February 2009.

[27] R. Schödel, T. Ott, R. Genzel, R. Hofmann, M. Lehnert, A. Eckart, N. Mouawad, T. Alexander, M. J. Reid, R. Lenzen, M. Hartung, F. Lacombe, D. Rouan, E. Gendron, G. Rousset, A.-M. Lagrange, W. Brandner, N. Ageorges, C. Lidman, A. F. M. Moorwood, J. Spyromilio, N. Hubin, and K. M. Menten. A star in a 15.2-year orbit around the supermassive black hole at the centre of the Milky Way. Nature, 419:694–696, October 2002.

[28] S. Gillessen, F. Eisenhauer, T. K. Fritz, H. Bartko, K. Dodds-Eden, O. Pfuhl, T. Ott, and R. Genzel. The Orbit of the Star S2 Around SGR A* from Very Large Telescope and Keck Data. ApJ, 707:L114–L117, December 2009.

[29] L. Meyer, A. M. Ghez, R. Schdel, S. Yelda, A. Boehle, J. R. Lu, T. Do, M. R. Morris, E. E. Becklin, and K. Matthews. The Shortest-Known Period Star Orbiting Our Galaxy's Supermassive Black Hole. *Science*, 338:84–, October 2012.

[30] K. M. Menten, M. J. Reid, A. Eckart, and R. Genzel. The Position of Sagittarius A*: Accurate

Alignment of the Radio and Infrared Reference Frames at the Galactic Center. ApJ, 475:L111, February 1997.

[31] F. Eisenhauer, R. Schdel, R. Genzel, T. Ott, M. Tecza, R. Abuter, A. Eckart, and T. Alexander. A Geometric Determination of the Distance to the Galactic Center. ApJ, 597:L121–L124, November 2003.

[32] M. Reid, K. M. Menten, and A. et al. Brunthaler. Trigonometric parallaxes of high mass star forming regions: the structure and kinematics of the milky way. ApJ, submitted, 2013.

[33] M. J. Reid, A. C. S. Readhead, R. C. Vermeulen, and R. N. Treuhaft. The Proper Motion of Sagittarius A*. I. First VLBA Results. ApJ, 524:816–823, October 1999.

[34] M. J. Reid and A. Brunthaler. The Proper Motion of Sagittarius A*. II. The Mass of Sagittarius A*. ApJ, 616:872–884, December 2004.

[35] S. Dibi, S. Markoff, R. Belmont, J. Malzac, N. Barrière, and J. Tomsick. Exploring plasma evolution during Sgr A* flares. MNRAS, subm., April 2013.

[36] H. Falcke, W. M. Goss, H. Matsuo, P. Teuben, J. H. Zhao, and R. Zylka. The Simultaneous Spectrum of Sagittarius A * from 20 Centimeters to 1 Millimeter and the Nature of the Millimeter Excess. ApJ, 499:731, May 1998.

[37] J.-H. Zhao, K. H. Young, R. M. Herrnstein, P. T. P. Ho, T. Tsutsumi, K. Y. Lo, W. M. Goss, and G. C. Bower. Variability of Sagittarius A*: Flares at 1 Millimeter. ApJ, 586:L29–L32, March 2003.

[38] E. Serabyn, J. Carlstrom, O. Lay, D. C. Lis, T. R. Hunter, and J. H. Lacy. High Frequency Measurements of the Spectrum of Sgr A*. ApJ, 490:L77–, November 1997.

[39] S. D. Hornstein, A. M. Ghez, A. Tanner, M. Morris, E. E. Becklin, and P. Wizinowich. Limits on the Short-Term Variability of Sagittarius A* in the Near-Infrared. ApJ, 577:L9–L13, September 2002.

[40] F. K. Baganoff, Y. Maeda, M. Morris, M. W. Bautz, W. N. Brandt, W. Cui, J. P. Doty, E. D. Feigelson, G. P. Garmire, S. H. Pravdo, G. R. Ricker, and L. K. Townsley. Chandra X-Ray Spectroscopic Imaging of Sagittarius A* and the Central Parsec of the Galaxy. ApJ, 591:891–915, July 2003.

[41] J. Neilsen, M. A. Nowak, C. Gammie, S. Nayakshin, S. Markoff, et al. A Chandra/HETGS census of X-ray variability from Sgr A* during 2012 . ApJ, in press, 2013.

[42] R. Schödel, M. R. Morris, K. Muzic, A. Alberdi, L. Meyer, A. Eckart, and D. Y. Gezari. The mean infrared emission of Sagittarius A*. A&A, 532:A83, August 2011.

[43] A. M. Ghez, S. A. Wright, K. Matthews, D. Thompson, D. Le Mignant, A. Tanner, S. D. Hornstein, M. Morris, E. E. Becklin, and B. T. Soifer. Variable Infrared Emission from the Supermassive Black Hole at the Center of the Milky Way. ApJ, 601:L159–L162, February 2004.

[44] R. Genzel, R. Schdel, T. Ott, A. Eckart, T. Alexander, F. Lacombe, D. Rouan, and B. Aschenbach. Near-infrared flares from accreting gas around the supermassive black hole at the Galactic Centre. Nature, 425:934–937, October 2003.

[45] K. Dodds-Eden, S. Gillessen, T. K. Fritz, F. Eisenhauer, S. Trippe, R. Genzel, T. Ott, H. Bartko, O. Pfuhl, G. Bower, A. Goldwurm, D. Porquet, G. Trap, and F. Yusef-Zadeh. The Two States of Sgr A* in the Near-infrared: Bright Episodic Flares on Top of Low-level Continuous Variability. ApJ, 728:37, February 2011.

[46] M. Bremer, G. Witzel, A. Eckart, M. Zamaninasab, R. M. Buchholz, R. Schödel, C. Straubmeier, M. García-Marín, and W. Duschl. The near-infrared spectral index of Sagittarius A* derived from Ks- and H-band flare statistics. A&A, 532:A26, August 2011.

[47] M. A. Nowak, J. Neilsen, S. B. Markoff, F. K. Baganoff, D. Porquet, N. Grosso, Y. Levin, J. Houck, A. Eckart, H. Falcke, L. Ji, J. M. Miller, and Q. D. Wang. Chandra/HETGS Observations of the Brightest Flare Seen from Sgr A*. ApJ, 759:95, November 2012.

[48] N.M. Barrièrre, J. A. Tomsick, F.K. Baganoff, S.E. Boggs, F.E. Christensen, et al. NuSTAR detection of high-energy X-ray emission and rapid variability from Sagittarius A* flares. ApJ,

subm., April 2013.

[49] S. Roy and A. Pramesh Rao. Sgr A* at low radio frequencies: Giant Metrewave Radio Telescope observations. MNRAS, 349:L25–L29, April 2004.

[50] M. E. Nord, T. J. W. Lazio, N. E. Kassim, W. M. Goss, and N. Duric. Detection of Sagittarius A* at 330 MHz with the Very Large Array. ApJ, 601:L51–L54, January 2004.

[51] R. Zylka and P. G. Mezger. Observations of SGR A West and SGR A* at the 1.3 MM wavelength. A&A, 190:L25–L28, January 1988.

[52] P. G. Mezger, R. Zylka, C. J. Salter, J. E. Wink, R. Chini, E. Kreysa, and R. Tuffs. Continuum observations of SGR A at mm/submm wavelengths. A&A, 209:337–348, January 1989.

[53] H. Falcke and P. L. Biermann. The Galactic Center - an AGN on a Starvation Diet. In I. Shlosman, editor, *Mass-Transfer Induced Activity in Galaxies*, page 44, 1994.

[54] R. D. Davies, D. Walsh, and R. S. Booth. The radio source at the galactic nucleus. MNRAS, 177:319–333, November 1976.

[55] K. Y. Lo, D. C. Backer, R. D. Ekers, K. I. Kellermann, M. Reid, and J. M. Moran. On the size of the galactic centre compact radio source: diameter less than 20 AU. Nature, 315:124–126, May 1985.

[56] K. Y. Lo, Z. Q. Shen, J. H. Zhao, and P. T. P. Ho. Intrinsic Size of Sagittarius A*: 72 Schwarzschild Radii. ApJ, 508:L61–L64, November 1998.

[57] G. C. Bower, W. M. Goss, H. Falcke, D. C. Backer, and Y. Lithwick. The Intrinsic Size of Sagittarius A* from 0.35 to 6 cm. ApJ, 648:L127–L130, September 2006.

[58] R. P. Eatough, H. Falcke, R. Karuppusamy, and et al. Revealing a high magnetic field around the supermassive black hole at the centre of the galaxy. Nature, page doi:10.1038/nature12499, 2013.

[59] L. G. Spitler, K. J. Lee, R. P. Eatough, M. Kramer, R. Karuppusamy, C. G. Bassa, I. Cognard, G. Desvignes, A. G. Lyne, B. W. Stappers, G. C. Bower, J. M. Cordes, D. J. Champion, and H. Falcke. Pulse Broadening Measurements from the Galactic Center Pulsar J1745–2900. *ArXiv e-prints*, September 2013.

[60] G. C. Bower, A. Deller, P. Demorest, A. Brunthaler, R. Eatough, H. Falcke, M. Kramer, K. J. Lee, and L. Spitler. The Angular Broadening of the Galactic Center Pulsar SGR J1745-29: A New Constraint on the Scattering Medium. *ArXiv e-prints*, September 2013.

[61] H. Falcke, S. Markoff, and G. C. Bower. Jet-lag in Sagittarius A*: what size and timing measurements tell us about the central black hole in the Milky Way. A&A, 496:77–83, March 2009.

[62] G. C. Bower, H. Falcke, R. M. Herrnstein, J.-H. Zhao, W. M. Goss, and D. C. Backer. Detection of the Intrinsic Size of Sagittarius A* Through Closure Amplitude Imaging. *Science*, 304:704–708, April 2004.

[63] Z.-Q. Shen, K. Y. Lo, M.-C. Liang, P. T. P. Ho, and J.-H. Zhao. A size of 1AU for the radio source Sgr A* at the centre of the Milky Way. Nature, 438:62–64, November 2005.

[64] S. S. Doeleman, J. Weintroub, A. E. E. Rogers, R. Plambeck, R. Freund, R. P. J. Tilanus, P. Friberg, L. M. Ziurys, J. M. Moran, B. Corey, K. H. Young, D. L. Smythe, M. Titus, D. P. Marrone, R. J. Cappallo, D. C.-J. Bock, G. C. Bower, R. Chamberlin, G. R. Davis, T. P. Krichbaum, J. Lamb, H. Maness, A. E. Niell, A. Roy, P. Strittmatter, D. Werthimer, A. R. Whitney, and D. Woody. Event-horizon-scale structure in the supermassive black hole candidate at the Galactic Centre. Nature, 455:78–80, September 2008.

[65] F. Yusef-Zadeh, M. Wardle, D. A. Roberts, C. O. Heinke, C. D. Dowell, W. D. Cotton, G. C. Bower, and F. K. Baganoff. Flaring Activity of SgrA*: Adiabatic Expansion of Nonthermal Plasma. In *Bulletin of the American Astronomical Society*, volume 38 of *Bulletin of the American Astronomical Society*, pages 1062–, December 2006.

[66] D. Maitra, S. Markoff, and H. Falcke. A time-dependent jet model for the emission from Sagittarius A*. A&A, 508:L13–L16, December 2009.

[67] A. Miyazaki, T. Tsutsumi, and M. Tsuboi. Intraday Variation of Sagittarius A* at Short

Millimeter Wavelengths. ApJ, 611:L97–L100, August 2004.

[68] J. C. Mauerhan, M. Morris, F. Walter, and F. K. Baganoff. Intraday Variability of Sagittarius A* at 3 Millimeters. ApJ, 623:L25–L28, April 2005.

[69] D. P. Marrone, F. K. Baganoff, M. R. Morris, J. M. Moran, A. M. Ghez, S. D. Hornstein, C. D. Dowell, D. J. Muoz, M. W. Bautz, G. R. Ricker, W. N. Brandt, G. P. Garmire, J. R. Lu, K. Matthews, J.-H. Zhao, R. Rao, and G. C. Bower. An X-Ray, Infrared, and Submillimeter Flare of Sagittarius A*. ApJ, 682:373–383, July 2008.

[70] R.-S. Lu, T. P. Krichbaum, A. Eckart, S. Knig, D. Kunneriath, G. Witzel, A. Witzel, and J. A. Zensus. Multiwavelength VLBI observations of Sagittarius A*. A&A, 525:A76, January 2011.

[71] F. Yusef-Zadeh, D. Roberts, M. Wardle, C. O. Heinke, and G. C. Bower. Flaring Activity of Sagittarius A* at 43 and 22 GHz: Evidence for Expanding Hot Plasma. ApJ, 650:189–194, October 2006.

[72] R. F. Coker and F. Melia. Hydrodynamical accretion onto sagittarius a* from distributed point sources. ApJ, 488:L149, October 1997.

[73] R. Genzel, D. Hollenbach, and C. H. Townes. The nucleus of our Galaxy. *Reports on Progress in Physics*, 57:417–479, May 1994.

[74] L. M. Ozernoy. Constraints on and Alternatives to a Massive Black Hole at the Galactic Center (review). In M. Morris, editor, *The Center of the Galaxy*, volume 136 of *IAU Symposium*, page 555, 1989.

[75] H. Bondi and F. Hoyle. On the mechanism of accretion by stars. MNRAS, 104:273, 1944.

[76] F. Melia. An accreting black hole model for Sagittarius A. ApJ, 387:L25–L28, March 1992.

[77] E. Quataert and A. Gruzinov. Convection-dominated Accretion Flows. ApJ, 539:809–814, August 2000.

[78] R. D. Blandford and M. C. Begelman. On the fate of gas accreting at a low rate on to a black hole. MNRAS, 303:L1–L5, February 1999.

[79] G. C. Bower, D. C. Backer, J.-H. Zhao, M. Goss, and H. Falcke. The Linear Polarization of Sagittarius A*. I. VLA Spectropolarimetry at 4.8 and 8.4 GHZ. ApJ, 521:582–586, August 1999.

[80] G. C. Bower, M. C. H. Wright, D. C. Backer, and H. Falcke. The Linear Polarization of Sagittarius A*. II. VLA and BIMA Polarimetry at 22, 43, and 86 GHz. ApJ, 527:851–855, December 1999.

[81] G. C. Bower, H. Falcke, and D. C. Backer. Detection of Circular Polarization in the Galactic Center Black Hole Candidate Sagittarius A*. ApJ, 523:L29–L32, September 1999.

[82] T. Beckert and H. Falcke. Circular polarization of radio emission from relativistic jets. A&A, 388:1106–1119, June 2002.

[83] G. C. Bower, H. Falcke, R. J. Sault, and D. C. Backer. The Spectrum and Variability of Circular Polarization in Sagittarius A* from 1.4 to 15 GHz. ApJ, 571:843–855, June 2002.

[84] D. J. Muoz, D. P. Marrone, J. M. Moran, and R. Rao. The Circular Polarization of Sagittarius A* at Submillimeter Wavelengths. ApJ, 745:115, February 2012.

[85] E. Agol. Sagittarius A* Polarization: No Advection-dominated Accretion Flow, Low Accretion Rate, and Nonthermal Synchrotron Emission. ApJ, 538:L121–L124, August 2000.

[86] T. A. Enßlin. Does circular polarisation reveal the rotation of quasar engines? A&A, 401:499–504, April 2003.

[87] L. Huang and R. V. Shcherbakov. Faraday conversion and rotation in uniformly magnetized relativistic plasmas. MNRAS, 416:2574–2592, October 2011.

[88] R. V. Shcherbakov, R. F. Penna, and J. C. McKinney. Sagittarius A* Accretion Flow and Black Hole Parameters from General Relativistic Dynamical and Polarized Radiative Modeling. ApJ, 755:133, August 2012.

[89] D. K. Aitken, J. Greaves, A. Chrysostomou, T. Jenness, W. Holland, J. H. Hough, D. Pierce-Price, and J. Richer. Detection of Polarized Millimeter and Submillimeter Emission from Sagittarius A*. ApJ, 534:L173–L176, May 2000.

[90] G. C. Bower, M. C. H. Wright, H. Falcke, and D. C. Backer. Interferometric Detection of Linear

Polarization from Sagittarius A* at 230 GHz. ApJ, 588:331–337, May 2003.

[91] G. C. Bower, H. Falcke, M. C. Wright, and D. C. Backer. Variable Linear Polarization from Sagittarius A*: Evidence of a Hot Turbulent Accretion Flow. ApJ, 618:L29–L32, January 2005.

[92] D. P. Marrone, J. M. Moran, J.-H. Zhao, and R. Rao. Interferometric Measurements of Variable 340 GHz Linear Polarization in Sagittarius A*. ApJ, 640:308–318, March 2006.

[93] J.-P. Macquart, G. C. Bower, M. C. H. Wright, D. C. Backer, and H. Falcke. The Rotation Measure and 3.5 Millimeter Polarization of Sagittarius A*. ApJ, 646:L111–L114, August 2006.

[94] D. P. Marrone, J. M. Moran, J.-H. Zhao, and R. Rao. An Unambiguous Detection of Faraday Rotation in Sagittarius A*. ApJ, 654:L57–L60, January 2007.

[95] P. Sharma, E. Quataert, and J. M. Stone. Faraday Rotation in Global Accretion Disk Simulations: Implications for Sgr A*. ApJ, 671:1696–1707, December 2007.

[96] Q.D. Wang, M. A. Nowak, S. Markoff, F. K. Baganoff, S. Nayakshin, F. Yuan, et al. Anatomy of X-ray-emitting gas around Sgr A*. *Science*, in press, 2013.

[97] R. M. Shannon and S. Johnston. Radio properties of the magnetar near Sagittarius A* from observations with the Australia Telescope Compact Array. *ArXiv e-prints*, May 2013.

[98] S. Gillessen, R. Genzel, T. K. Fritz, E. Quataert, C. Alig, A. Burkert, J. Cuadra, F. Eisenhauer, O. Pfuhl, K. Dodds-Eden, C. F. Gammie, and T. Ott. A gas cloud on its way towards the supermassive black hole at the Galactic Centre. Nature, 481:51–54, January 2012.

[99] S. Gillessen, R. Genzel, T. K Fritz, F. Eisenhauer, O. Pfuhl, T. Ott, M. Schartmann, A. Ballone, and A. Burkert. Pericenter passage of the gas cloud G2 in the Galactic Center. ApJ, 774:44, June 2013.

[100] A. Burkert, M. Schartmann, C. Alig, S. Gillessen, R. Genzel, T. K. Fritz, and F. Eisenhauer. Physics of the Galactic Center Cloud G2, on Its Way toward the Supermassive Black Hole. ApJ, 750:58, May 2012.

[101] Peter Anninos, P Chris Fragile, Julia Wilson, and Stephen D Murray. Three-dimensional moving-mesh simulations of galactic center cloud g2. ApJ, 759(2):132, 2012.

[102] F. K. Baganoff, M. W. Bautz, W. N. Brandt, G. Chartas, E. D. Feigelson, G. P. Garmire, Y. Maeda, M. Morris, G. R. Ricker, L. K. Townsley, and F. Walter. Rapid X-ray flaring from the direction of the supermassive black hole at the Galactic Centre. Nature, 413:45–48, September 2001.

[103] R. Genzel, R. Schödel, T. Ott, A. Eckart, T. Alexander, F. Lacombe, D. Rouan, and B. Aschenbach. Near-infrared flares from accreting gas around the supermassive black hole at the Galactic Centre. Nature, 425:934–937, October 2003.

[104] T. Do, A. M. Ghez, M. R. Morris, S. Yelda, L. Meyer, J. R. Lu, S. D. Hornstein, and K. Matthews. A Near-Infrared Variability Study of the Galactic Black Hole: A Red Noise Source with NO Detected Periodicity. ApJ, 691:1021–1034, February 2009.

[105] G. Witzel, A. Eckart, M. Bremer, M. Zamaninasab, B. Shahzamanian, M. Valencia-S., R. Schödel, V. Karas, R. Lenzen, N. Marchili, N. Sabha, M. Garcia-Marin, R. M. Buchholz, D. Kunneriath, and C. Straubmeier. Source-intrinsic Near-infrared Properties of Sgr A*: Total Intensity Measurements. ApJS, 203:18, December 2012.

[106] C. R. Canizares, J. E. Davis, D. Dewey, K. A. Flanagan, E. B. Galton, D. P. Huenemoerder, K. Ishibashi, T. H. Markert, H. L. Marshall, M. McGuirk, M. L. Schattenburg, N. S. Schulz, H. I. Smith, and M. Wise. The Chandra High-Energy Transmission Grating: Design, Fabrication, Ground Calibration, and 5 Years in Flight. PASP, 117:1144–1171, October 2005.

[107] N. M. Nagar, H. Falcke, and A. S. Wilson. Radio sources in low-luminosity active galactic nuclei. IV. Radio luminosity function, importance of jet power, and radio properties of the complete Palomar sample. A&A, 435:521–543, May 2005.

[108] J. N. Clarke. Extraterrestrial intelligence and galactic nuclear activity. Icarus, 46:94–96, April 1981.

[109] X. Haubois, K. Dodds-Eden, A. Weiss, T. Paumard, G. Perrin, Y. Clnet, S. Gillessen, P. Kervella,

      F. Eisenhauer, R. Genzel, and D. Rouan. Flares and variability from Sagittarius A*: five nights of simultaneous multi-wavelength observations. A&A, 540:A41, April 2012.

[110] R. Narayan and I. Yi. Advection-dominated Accretion: Underfed Black Holes and Neutron Stars. ApJ, 452:710+, October 1995.

[111] R. Narayan, R. Mahadevan, J. E. Grindlay, R. G. Popham, and C. Gammie. Advection-dominated accretion model of sagittarius a*: evidence for a black hole at the galactic center. ApJ, 492:554–568, January 1998.

[112] H. Falcke, K. Mannheim, and P. L. Biermann. The galactic center radio jet. A&A, 278:L1–L4, October 1993.

[113] H. Falcke and S. Markoff. The jet model for Sgr A*: Radio and X-ray spectrum. A&A, 362:113–118, October 2000.

[114] M. Mocibrodzka, C. F. Gammie, J. C. Dolence, H. Shiokawa, and P. K. Leung. Radiative Models of SGR A* from GRMHD Simulations. ApJ, 706:497–507, November 2009.

[115] S. Dibi, S. Drappeau, P. C. Fragile, S. Markoff, and J. Dexter. General relativistic magnetohydrodynamic simulations of accretion on to Sgr A*: how important are radiative losses? MNRAS, 426:1928–1939, November 2012.

[116] S. Drappeau, S. Dibi, J. Dexter, S. Markoff, and P. C. Fragile. Self-consistent spectra from radiative GRMHD simulations of accretion on to Sgr A*. MNRAS, 431:2872–2884, May 2013.

[117] R. V. Shcherbakov and F. K. Baganoff. Inflow-Outflow Model with Conduction and Self-consistent Feeding for Sgr A*. ApJ, 716:504–509, June 2010.

[118] S. P. Reynolds and C. F. McKee. The compact radio source at the galactic center. ApJ, 239:893–897, August 1980.

[119] R. D. Blandford and A. Königl. Relativistic jets as compact radio sources. ApJ, 232:34–48, August 1979.

[120] H. Falcke and P. L. Biermann. The jet-disk symbiosis. I. Radio to X-ray emission models for quasars. A&A, 293:665–682, January 1995.

[121] H. Falcke. The Jet Model for SGR A*. In H. Falcke, A. Cotera, W.J. Duschl, F. Melia, and M. J. Rieke, editors, *ASP Conf. Ser. 186: The Central Parsecs of the Galaxy*, page 148, San Francisco, June 1999. Astronomical Society of the Pacific.

[122] S. Markoff, H. Falcke, F. Yuan, and P. L. Biermann. The Nature of the 10 kilosecond X-ray flare in Sgr A*. A&A, 379:L13–L16, November 2001.

[123] H. Falcke, S. Markoff, and G. C. Bower. Jet-lag in Sagittarius A*: what size and timing measurements tell us about the central black hole in the Milky Way. A&A, 496:77–83, March 2009.

[124] D. L. Meier. The Association of Jet Production with Geometrically Thick Accretion Flows and Black Hole Rotation. ApJ, 548:L9–L12, February 2001.

[125] K. Beckwith, J. F. Hawley, and J. H. Krolik. The Influence of Magnetic Field Geometry on the Evolution of Black Hole Accretion Flows: Similar Disks, Drastically Different Jets. ApJ, 678:1180–1199, May 2008.

[126] J. C. McKinney. General relativistic magnetohydrodynamic simulations of the jet formation and large-scale propagation from black hole accretion systems. MNRAS, 368:1561–1582, June 2006.

[127] M. Moscibrodzka and H. Falcke. A coupled jet-disk model for Sgr A*: explaining the flat-spectrum radio core with GRMHD simulations of jets. A&A, in press, 2013.

[128] Z. Li, M. R. Morris, and F. K. Baganoff. Evidence for A Parsec-scale Jet from The Galactic Center Black Hole: Interaction with Local Gas. ApJ, in press. (arXiv:1310.0146), April 2013.

[129] S. Markoff, G. C. Bower, and H. Falcke. How to hide large-scale outflows: size constraints on the jets of Sgr A*. MNRAS, 379:1519–1532, August 2007.

[130] F. Yuan, E. Quataert, and R. Narayan. Nonthermal Electrons in Radiatively Inefficient Accretion Flow Models of Sagittarius A*. ApJ, 598:301–312, November 2003.

[131] H. Falcke, E. Krding, and S. Markoff. A scheme to unify low-power accreting black holes. Jet-dominated accretion flows and the radio/X-ray correlation. A&A, 414:895–903, February 2004.

[132] A. Merloni, S. Heinz, and T. di Matteo. A Fundamental Plane of black hole activity. MNRAS, 345:1057–1076, November 2003.

[133] S. Markoff. Sagittarius A* in Context: Daily Flares as a Probe of the Fundamental X-Ray Emission Process in Accreting Black Holes. ApJ, 618:L103–L106, January 2005.

[134] R. M. Plotkin, S. Markoff, B. C. Kelly, E. Körding, and S. F. Anderson. Using the Fundamental Plane of black hole activity to distinguish X-ray processes from weakly accreting black holes. MNRAS, 419:267–286, January 2012.

[135] F. Yuan, S. Markoff, and H. Falcke. A Jet-ADAF model for Sgr A*. A&A, 383:854–863, March 2002.

[136] S. Liu, V. Petrosian, and F. Melia. Electron Acceleration around the Supermassive Black Hole at the Galactic Center. ApJ, 611:L101–L104, August 2004.

[137] F. Yuan, E. Quataert, and R. Narayan. On the Nature of the Variable Infrared Emission from Sagittarius A*. ApJ, 606:894–899, May 2004.

[138] K. Zubovas, S. Nayakshin, and S. Markoff. Sgr A* flares: tidal disruption of asteroids and planets? MNRAS, 421:1315–1324, April 2012.

[139] A. Eckart, F. K. Baganoff, M. Morris, M. W. Bautz, W. N. Brandt, G. P. Garmire, R. Genzel, T. Ott, G. R. Ricker, C. Straubmeier, T. Viehmann, R. Schödel, G. C. Bower, and J. E. Goldston. First simultaneous NIR/X-ray detection of a flare from Sgr A*. A&A, 427:1–11, November 2004.

[140] K. Dodds-Eden, D. Porquet, G. Trap, E. Quataert, X. Haubois, S. Gillessen, N. Grosso, E. Pantin, H. Falcke, D. Rouan, R. Genzel, G. Hasinger, A. Goldwurm, F. Yusef-Zadeh, Y. Clenet, S. Trippe, P.-O. Lagage, H. Bartko, F. Eisenhauer, T. Ott, T. Paumard, G. Perrin, F. Yuan, T. K. Fritz, and L. Mascetti. Evidence for X-Ray Synchrotron Emission from Simultaneous Mid-Infrared to X-Ray Observations of a Strong Sgr A* Flare. ApJ, 698:676–692, June 2009.

[141] G. C. Bower, S. Markoff, A. Brunthaler, C. Law, H. Falcke, D. Maitra, M. Clavel, A. Goldwurm, M. R. Morris, G. Witzel, L. Meyer, and A. M. Ghez. Detection of variability in the size of sagittarius a*. ApJ, page submitted, 2013.

[142] J. C. Dolence, C. F. Gammie, H. Shiokawa, and S. C. Noble. Near-infrared and X-Ray Quasi-periodic Oscillations in Numerical Models of Sgr A*. ApJ, 746:L10, February 2012.

[143] R. V. Shcherbakov and J. C. McKinney. Submillimeter Quasi-Periodic Oscillations in Magnetically Choked Accretion Flows Models of Sgr A*. ApJ, subm. (arXiv:1304.7768), April 2013.

[144] A. Ingram, C. Done, and P. C. Fragile. Low-frequency quasi-periodic oscillations spectra and Lense-Thirring precession. MNRAS, 397:L101–L105, July 2009.

[145] B. Aschenbach, N. Grosso, D. Porquet, and P. Predehl. X-ray flares reveal mass and angular momentum of the Galactic Center black hole. A&A, 417:71–78, April 2004.

[146] A. Eckart, F. K. Baganoff, M. Zamaninasab, M. R. Morris, R. Schdel, L. Meyer, K. Muzic, M. W. Bautz, W. N. Brandt, G. P. Garmire, G. R. Ricker, D. Kunneriath, C. Straubmeier, W. Duschl, M. Dovciak, V. Karas, S. Markoff, F. Najarro, J. Mauerhan, J. Moultaka, and A. Zensus. Polarized NIR and X-ray flares from Sagittarius A*. A&A, 479:625–639, March 2008.

[147] T. Johannsen and D. Psaltis. Testing the No-hair Theorem with Observations in the Electromagnetic Spectrum. III. Quasi-periodic Variability. ApJ, 726:11, January 2011.

[148] J. M. Bardeen. Timelike and null geodesics in the kerr metric. In C. DeWitt and B. S. DeWitt, editors, *Black Holes*, pages 215–239, New York, 1973. Gordon & Breach.

[149] N. I. Shakura and R. A. Sunyaev. Black holes in binary systems. observational appearance. A&A, 24:337–355, 1973.

[150] C. T. Cunningham. The effects of redshifts and focusing on the spectrum of an accretion disk around a kerr black hole. ApJ, 202:788–802, December 1975.

[151] J. M. Hollywood and F. Melia. The effects of redshifts and focusing on the spectrum of an accretion disk in the galactic center black hole candidate Sagittarius A*. ApJ, 443:L17–L20,

April 1995.

[152] S. U. Viergutz. Radiation from arbitrarily shaped objects in the vicinity of Kerr black holes. Ap&SS, 205:155–161, July 1993.

[153] A. de Vries. The apparent shape of a rotating charged black hole, closed photon orbits and the bifurcation set A_4. *Classical and Quantum Gravity*, 17:123–144, January 2000.

[154] T. Johannsen and D. Psaltis. Testing the No-hair Theorem with Observations in the Electromagnetic Spectrum. II. Black Hole Images. ApJ, 718:446–454, July 2010.

[155] A. B. Kamruddin and J. Dexter. A geometric crescent model for black hole images. MNRAS, July 2013.

[156] R. Takahashi. Shapes and Positions of Black Hole Shadows in Accretion Disks and Spin Parameters of Black Holes. ApJ, 611:996–1004, August 2004.

[157] A. E. Broderick and A. Loeb. Frequency-dependent Shift in the Image Centroid of the Black Hole at the Galactic Center as a Test of General Relativity. ApJ, 636:L109–L112, January 2006.

[158] K. Hioki and K.-I. Maeda. Measurement of the Kerr spin parameter by observation of a compact object's shadow. Phys. Rev. D, 80(2):024042, July 2009.

[159] C. Bambi, K. Freese, and R. Takahashi. Is the Carter-Israel conjecture correct? *ArXiv e-prints*, August 2009.

[160] A. E. Broderick and R. Narayan. On the Nature of the Compact Dark Mass at the Galactic Center. ApJ, 638:L21–L24, February 2006.

[161] A. E. Broderick, A. Loeb, and R. Narayan. The Event Horizon of Sagittarius A*. ApJ, 701:1357–1366, August 2009.

[162] C. Bambi and K. Freese. Apparent shape of super-spinning black holes. Phys. Rev. D, 79(4):043002, February 2009.

[163] D. F. Torres, S. Capozziello, and G. Lambiase. Supermassive boson star at the galactic center? Phys. Rev. D, 62(10):104012, November 2000.

[164] C. B. M. H. Chirenti and L. Rezzolla. How to tell a gravastar from a black hole. *Classical and Quantum Gravity*, 24:4191–4206, August 2007.

[165] C. Bambi. Can the supermassive objects at the centers of galaxies be traversable wormholes? The first test of strong gravity for mm/sub-mm very long baseline interferometry facilities. Phys. Rev. D, 87(10):107501, May 2013.

[166] E. F. Eiroa and C. M. Sendra. Gravitational lensing by massless braneworld black holes. Phys. Rev. D, 86(8):083009, October 2012.

[167] A. Abdujabbarov, F. Atamurotov, Y. Kucukakca, B. Ahmedov, and U. Camci. Shadow of Kerr-Taub-NUT black hole. Ap&SS, 344:429–435, April 2013.

[168] A. F. Zakharov, F. de Paolis, G. Ingrosso, and A. A. Nucita. Direct measurements of black hole charge with future astrometrical missions. A&A, 442:795–799, November 2005.

[169] F. Atamurotov, A. Abdujabbarov, and B. Ahmedov. Shadow of rotating Hoava-Lifshitz black hole. Ap&SS, July 2013.

[170] K. Hioki and U. Miyamoto. Hidden symmetries, null geodesics, and photon capture in the Sen black hole. Phys. Rev. D, 78(4):044007, August 2008.

[171] L. Amarilla and E. F. Eiroa. Shadow of a Kaluza-Klein rotating dilaton black hole. Phys. Rev. D, 87(4):044057, February 2013.

[172] C. Bambi and N. Yoshida. Shape and position of the shadow in the $\delta = 2$ Tomimatsu-Sato spacetime. *Classical and Quantum Gravity*, 27(20):205006, October 2010.

[173] A. F. Zakharov, F. D. Paolis, G. Ingrosso, and A. A. Nucita. Shadows as a tool to evaluate black hole parameters and a dimension of spacetime. New Astron. Rev., 56:64–73, February 2012.

[174] A. Yumoto, D. Nitta, T. Chiba, and N. Sugiyama. Shadows of multi-black holes: Analytic exploration. Phys. Rev. D, 86(10):103001, November 2012.

[175] M. J. Reid, A. E. Broderick, A. Loeb, M. Honma, and A. Brunthaler. Limits on the Position Wander of Sgr A*. ApJ, 682:1041–1046, August 2008.

[176] A. E. Broderick, V. L. Fish, S. S. Doeleman, and A. Loeb. Constraining the Structure of Sagittarius A*'s Accretion Flow with Millimeter Very Long Baseline Interferometry Closure Phases. ApJ, 738:38, September 2011.

[177] F. Yuan, Z.-Q. Shen, and L. Huang. Testing the Radiatively Inefficient Accretion Flow Model for Sagittarius A* Using the Size Measurements. ApJ, 642:L45–L48, May 2006.

[178] L. Huang, M. Cai, Z.-Q. Shen, and F. Yuan. Black hole shadow image and visibility analysis of Sagittarius A*. MNRAS, 379:833–840, August 2007.

[179] J. Dexter, E. Agol, P. C. Fragile, and J. C. McKinney. The Submillimeter Bump in Sgr A* from Relativistic MHD Simulations. ApJ, 717:1092–1104, July 2010.

[180] B. C. Bromley, F. Melia, and S. Liu. Polarimetric Imaging of the Massive Black Hole at the Galactic Center. ApJ, 555:L83–L86, July 2001.

[181] V. L. Fish, S. S. Doeleman, A. E. Broderick, A. Loeb, and A. E. E. Rogers. Detecting Changing Polarization Structures in Sagittarius A* with High Frequency VLBI. ApJ, 706:1353–1363, December 2009.

[182] L. Huang, S. Liu, Z.-Q. Shen, M. J. Cai, H. Li, and C. L. Fryer. Linearly and Circularly Polarized Emission in Sagittarius A*. ApJ, 676:L119–L122, April 2008.

[183] A. Broderick and R. Blandford. Covariant magnetoionic theory - I. Ray propagation. MNRAS, 342:1280–1290, July 2003.

[184] A. E. Broderick, V. L. Fish, S. S. Doeleman, and A. Loeb. Estimating the Parameters of Sagittarius A*'s Accretion Flow Via Millimeter VLBI. ApJ, 697:45–54, May 2009.

[185] S. S. Doeleman, V. L. Fish, A. E. Broderick, A. Loeb, and A. E. E. Rogers. Detecting Flaring Structures in Sagittarius A* with High-Frequency VLBI. ApJ, 695:59–74, April 2009.

[186] V. L. Fish, A. E. Broderick, S. S. Doeleman, and A. Loeb. Using Millimeter VLBI to Constrain RIAF Models of Sagittarius A*. ApJ, 692:L14–L18, February 2009.

[187] T. P. Krichbaum, D. A. Graham, A. Witzel, A. Greve, J. E. Wink, M. Grewing, F. Colomer, P. de Vicente, J. Gomez-Gonzalez, A. Baudry, and J. A. Zensus. VLBI observations of the galactic center source SGR A* at 86 GHz and 215 GHz. A&A, 335:L106–L110, July 1998.

[188] V. L. Fish, S. S. Doeleman, C. Beaudoin, R. Blundell, D. E. Bolin, G. C. Bower, R. Chamberlin, R. Freund, P. Friberg, M. A. Gurwell, M. Honma, M. Inoue, T. P. Krichbaum, J. Lamb, D. P. Marrone, J. M. Moran, T. Oyama, R. Plambeck, R. Primiani, A. E. E. Rogers, D. L. Smythe, J. SooHoo, P. Strittmatter, R. P. J. Tilanus, M. Titus, J. Weintroub, M. Wright, D. Woody, K. H. Young, and L. M. Ziurys. 1.3 mm Wavelength VLBI of Sagittarius A*: Detection of Time-variable Emission on Event Horizon Scales. ApJ, 727:L36, February 2011.

[189] V. L. Fish and S. S. Doeleman. Observing a black hole event horizon: (sub)millimeter VLBI of Sgr A*. In S. A. Klioner, P. K. Seidelmann, and M. H. Soffel, editors, IAU Symposium, volume 261 of IAU Symposium, pages 271–276, January 2010.

[190] H. Falcke, R. Laing, L. Testi, and A. Zensus. Report on the ESO Workshop "mm-wave VLBI with ALMA and Radio Telescopes around the World". The Messenger, 149:50–53, September 2012.

[191] T. P. Krichbaum, A. Roy, J. Wagner, H. Rottmann, J. A. Hodgson, A. Bertarini, W. Alef, J. A. Zensus, A. P. Marscher, S. G. Jorstad, R. Freund, D. Marrone, P. Strittmatter, L. Ziurys, R. Blundell, J. Weintroub, K. Young, V. Fish, S. Doeleman, M. Bremer, S. Sanchez, L. Fuhrmann, E. Angelakis, and V. Karamanavis. Zooming towards the Event Horizon - mm-VLBI today and tomorrow. ArXiv e-prints, May 2013.

[192] W. Cash. X-ray Interferometry. In J. Romney and M. Reid, editors, Future Directions in High Resolution Astronomy, volume 340 of Astronomical Society of the Pacific Conference Series, page 633, December 2005.

[193] F. Eisenhauer, G. Perrin, W. Brandner, C. Straubmeier, K. Perraut, A. Amorim, M. Schller, S. Gillessen, P. Kervella, M. Benisty, C. Araujo-Hauck, L. Jocou, J. Lima, G. Jakob, M. Haug, Y. Clnet, T. Henning, A. Eckart, J.-P. Berger, P. Garcia, R. Abuter, S. Kellner, T. Paumard, S. Hippler, S. Fischer, T. Moulin, J. Villate, G. Avila, A. Grter, S. Lacour, A. Huber, M. Wiest,

A. Nolot, P. Carvas, R. Dorn, O. Pfuhl, E. Gendron, S. Kendrew, S. Yazici, S. Anton, Y. Jung, M. Thiel, . Choquet, R. Klein, P. Teixeira, P. Gitton, D. Moch, F. Vincent, N. Kudryavtseva, S. Strbele, S. Sturm, P. Fdou, R. Lenzen, P. Jolley, C. Kister, V. Lapeyrre, V. Naranjo, C. Lucuix, R. Hofmann, F. Chapron, U. Neumann, L. Mehrgan, O. Hans, G. Rousset, J. Ramos, M. Suarez, R. Lederer, J.-M. Reess, R.-R. Rohloff, P. Haguenauer, H. Bartko, A. Sevin, K. Wagner, J.-L. Lizon, S. Rabien, C. Collin, G. Finger, R. Davies, D. Rouan, M. Wittkowski, K. Dodds-Eden, D. Ziegler, F. Cassaing, H. Bonnet, M. Casali, R. Genzel, and P. Lena. GRAVITY: Observing the Universe in Motion. *The Messenger*, 143:16–24, March 2011.

[194] N. Wex and S. M. Kopeikin. Frame Dragging and Other Precessional Effects in Black Hole Pulsar Binaries. ApJ, 514:388–401, March 1999.

[195] K. Liu, N. Wex, M. Kramer, J. M. Cordes, and T. J. W. Lazio. Prospects for Probing the Spacetime of Sgr A* with Pulsars. ApJ, 747:1, March 2012.

[196] R. S. Wharton, S. Chatterjee, J. M. Cordes, J. S. Deneva, and T. J. W. Lazio. Multiwavelength Constraints on Pulsar Populations in the Galactic Center. ApJ, 753:108, July 2012.

[197] M. Shibata and M. Sasaki. Innermost stable circular orbits around relativistic rotating stars. Phys. Rev. D, 58(10):104011, November 1998.

[198] M. Bursa, M. A. Abramowicz, V. Karas, W. Kluniak, and A. Schwarzenberg-Czerny. The timescale of encircling light. In S. Hledík and Z. Stuchlík, editors, *Proceedings of RAGtime 8/9: Workshops on Black Holes and Neutron Stars*, pages 21–25, December 2007.